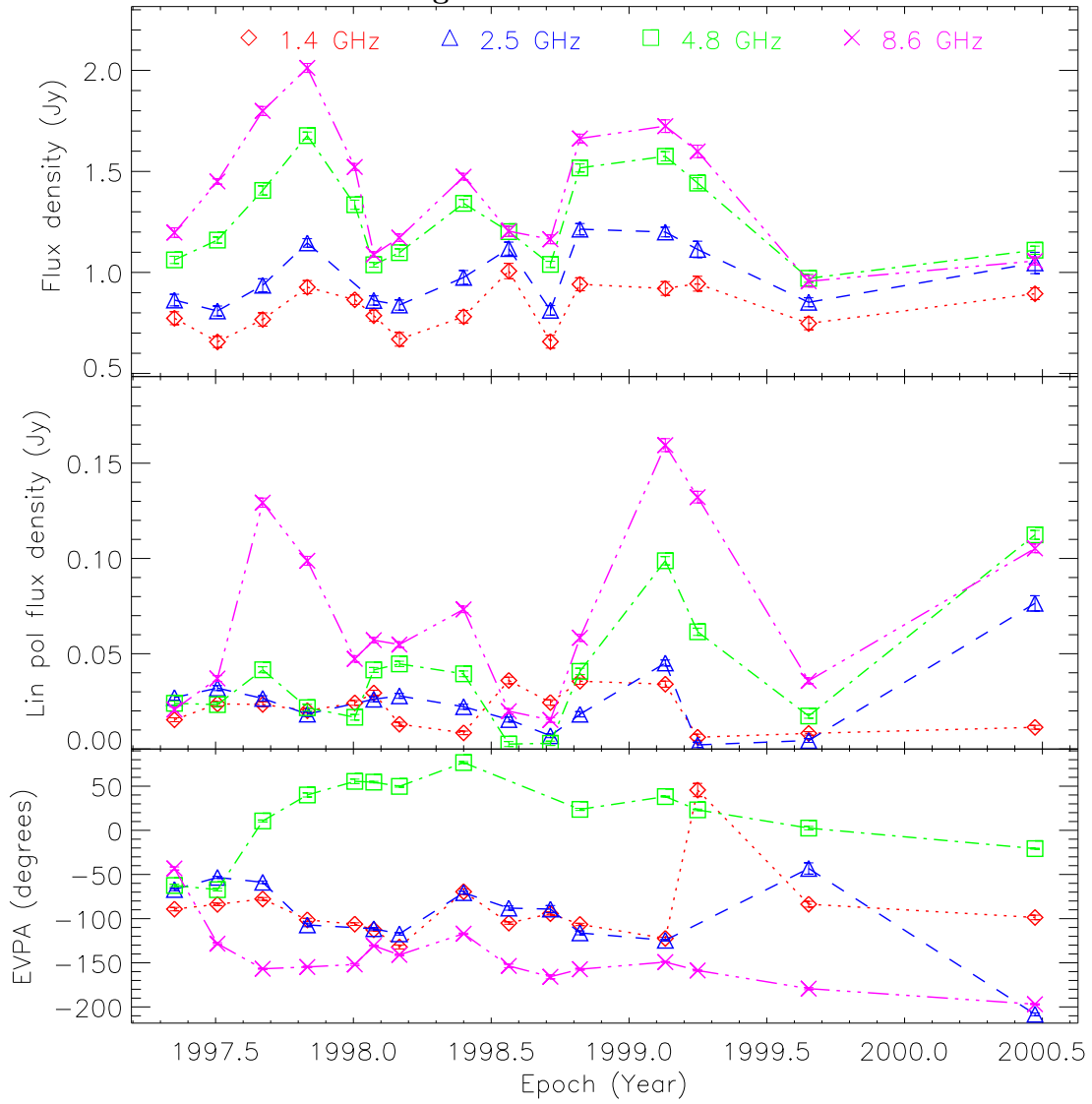


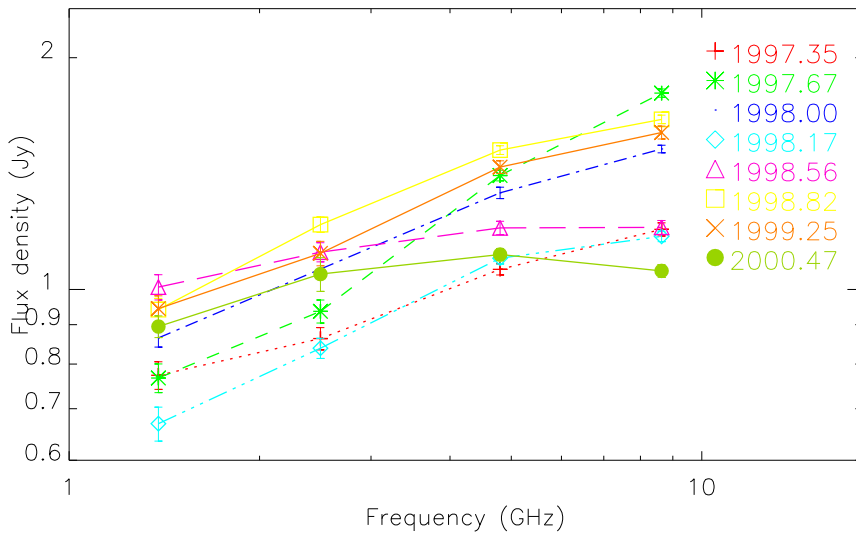
Appendix A

Long-term flux density monitoring data

Figure A.1: PKS 0048–097



0048–097



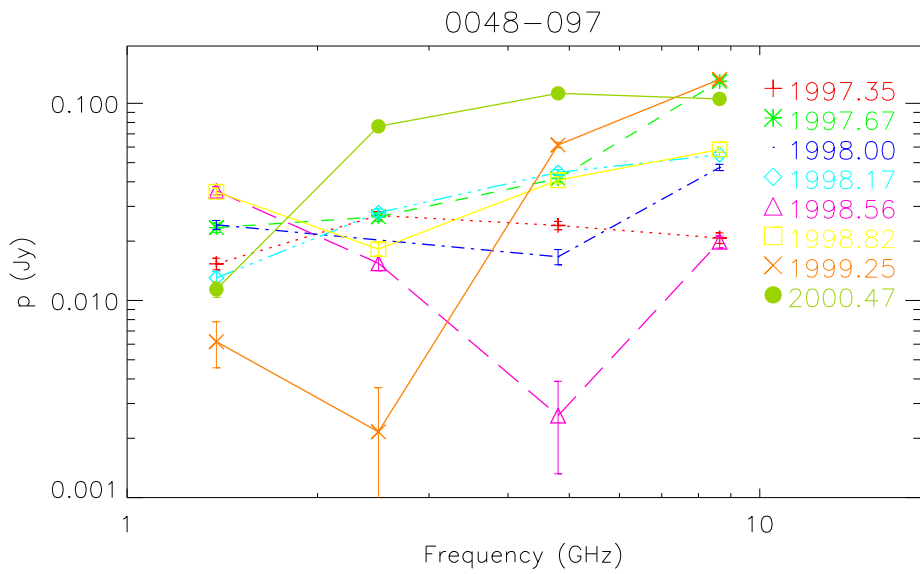
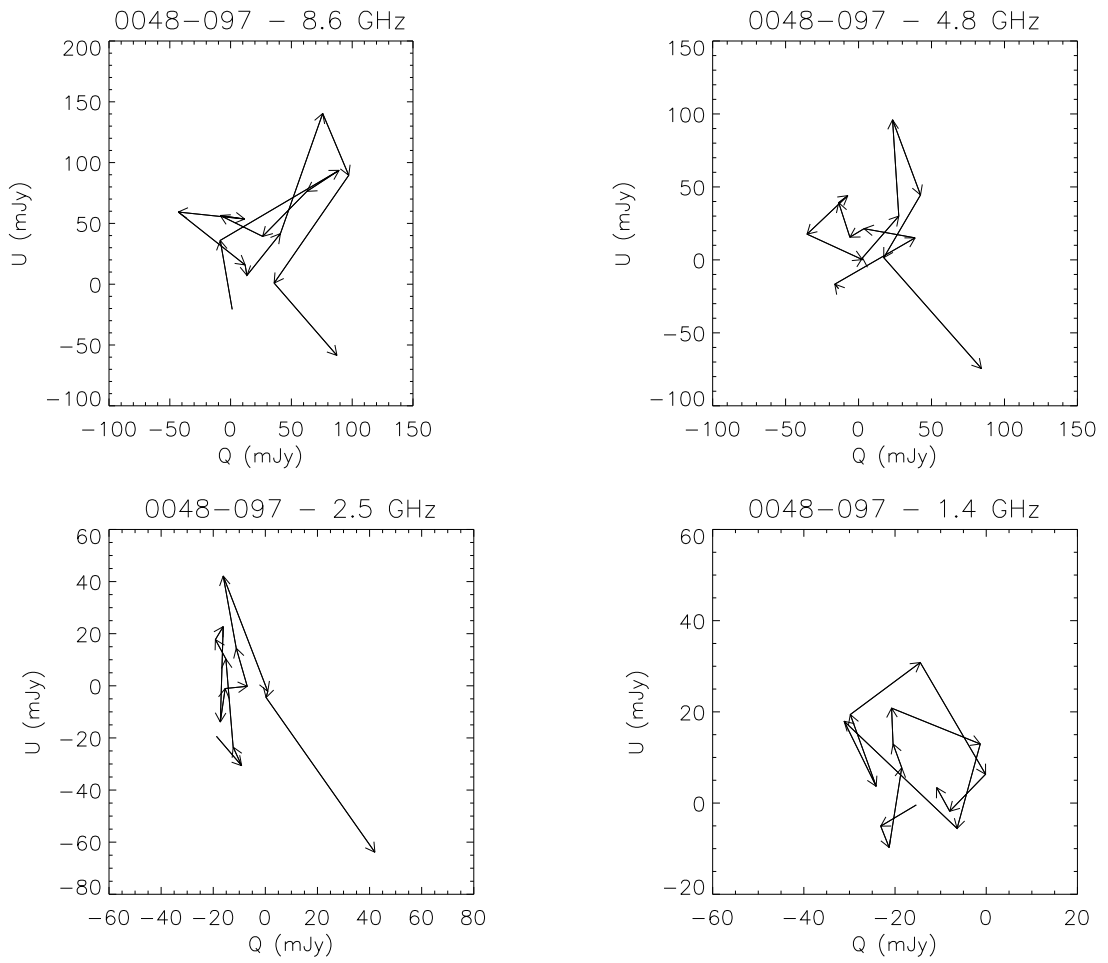
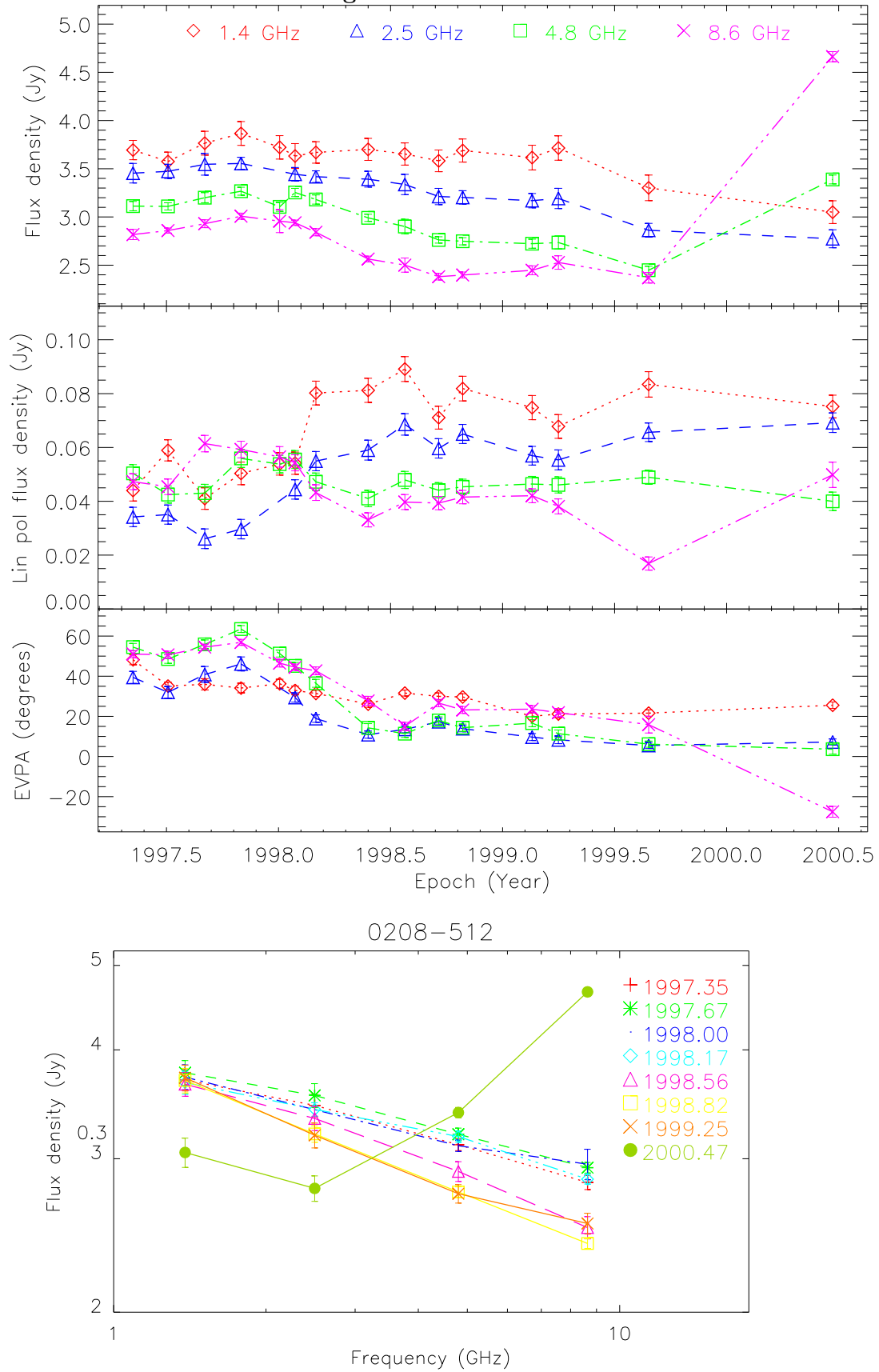


Figure A.2: PKS 0208–512



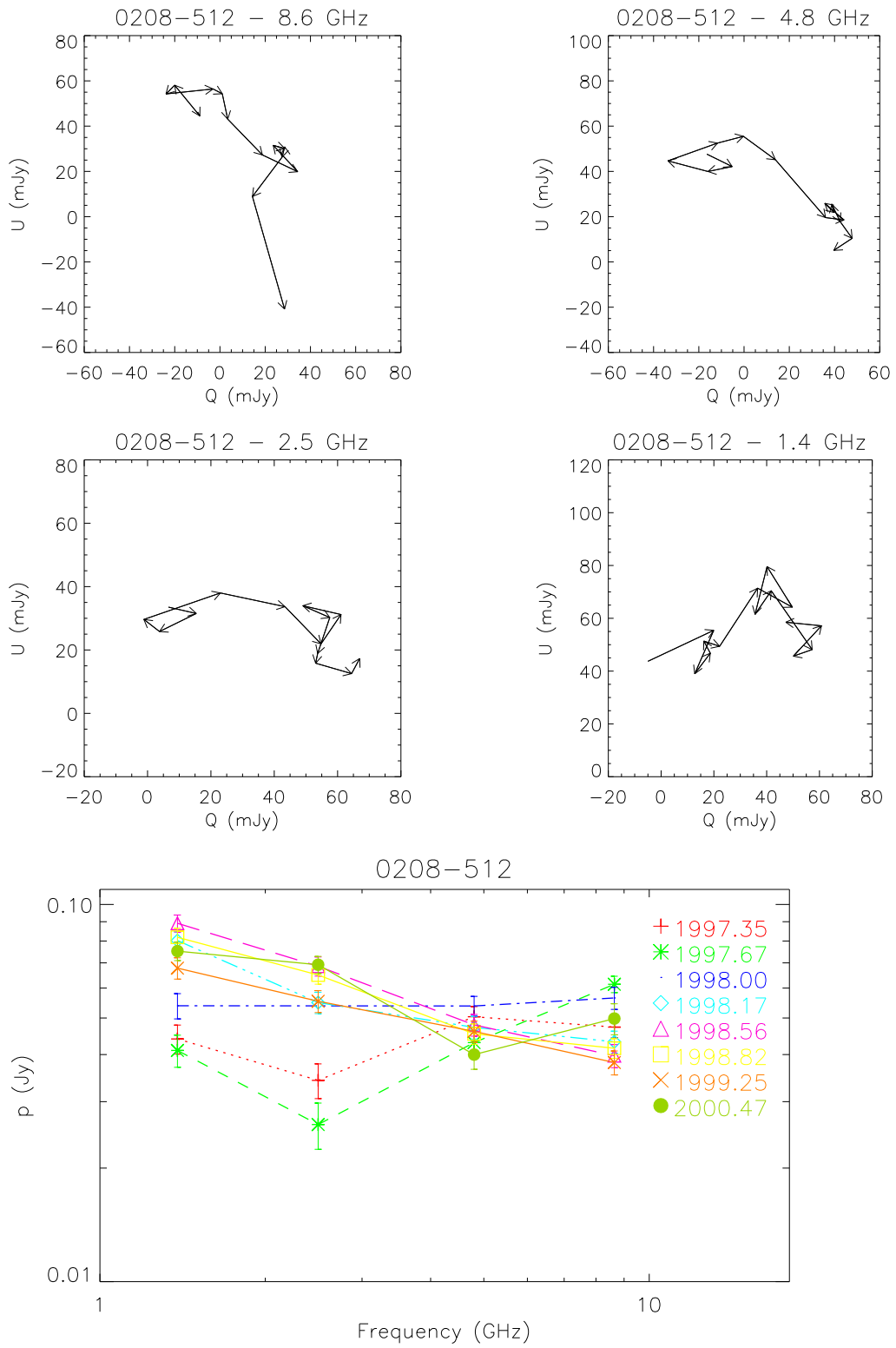
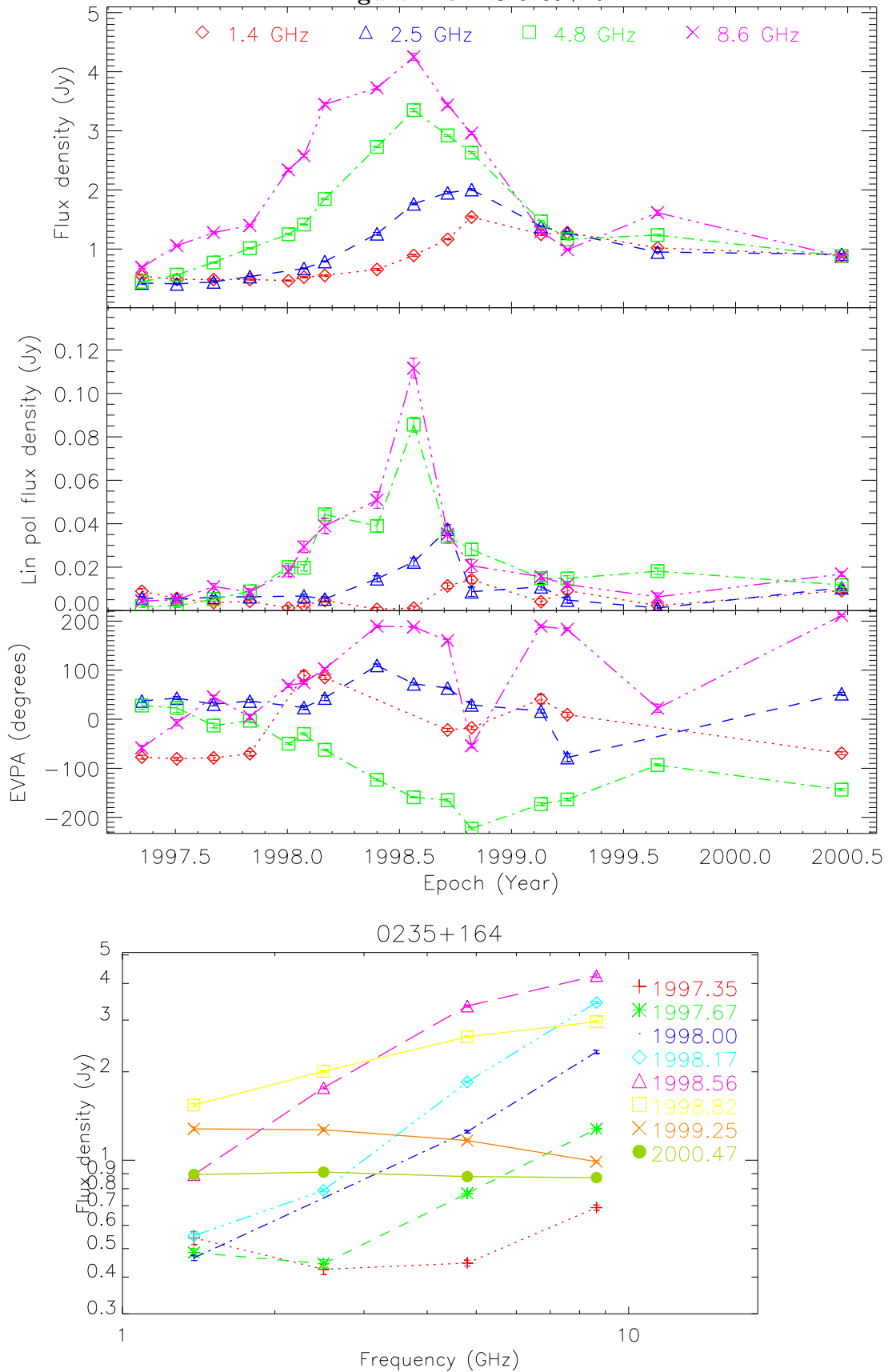


Figure A.3: AO 0235+164



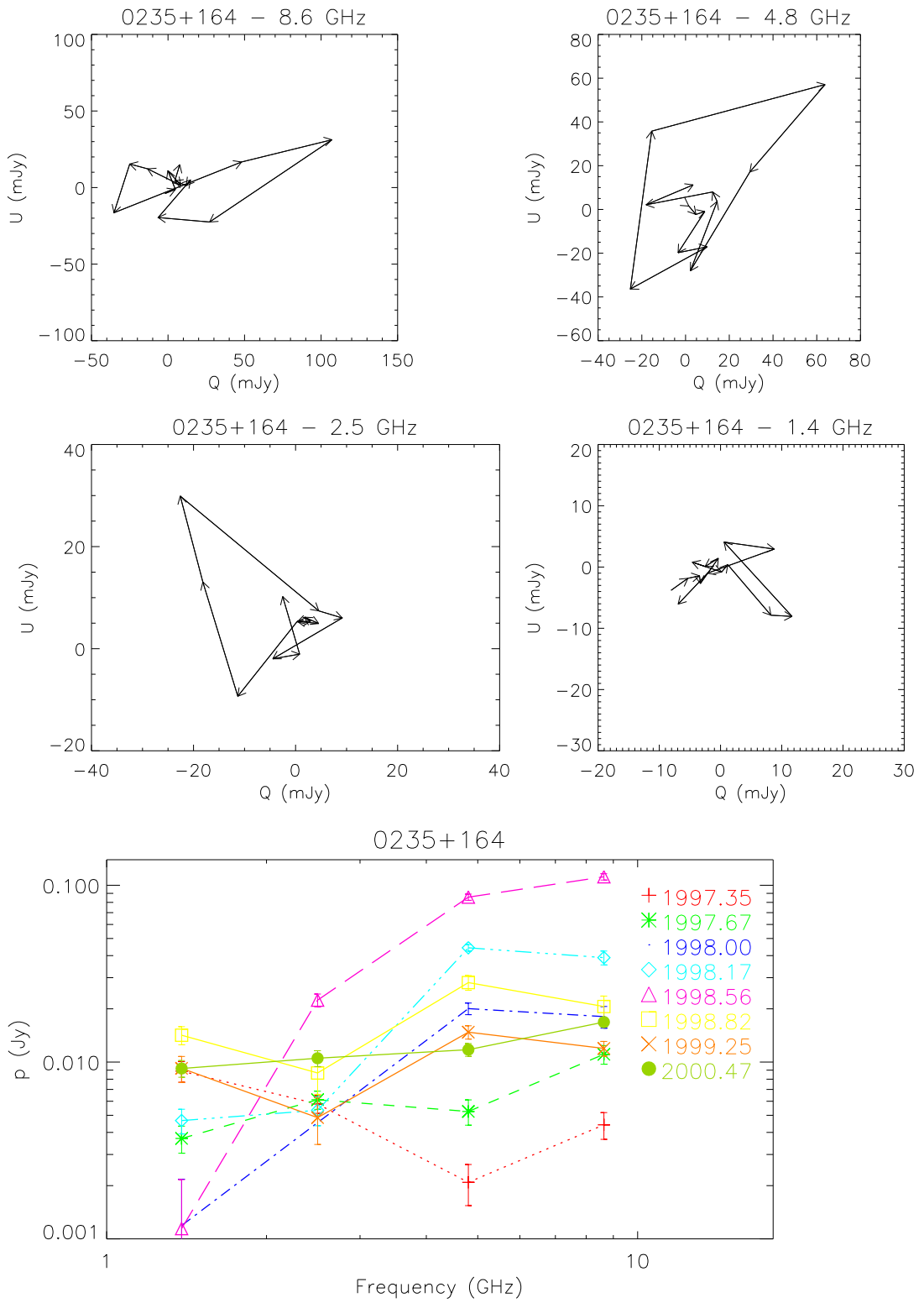
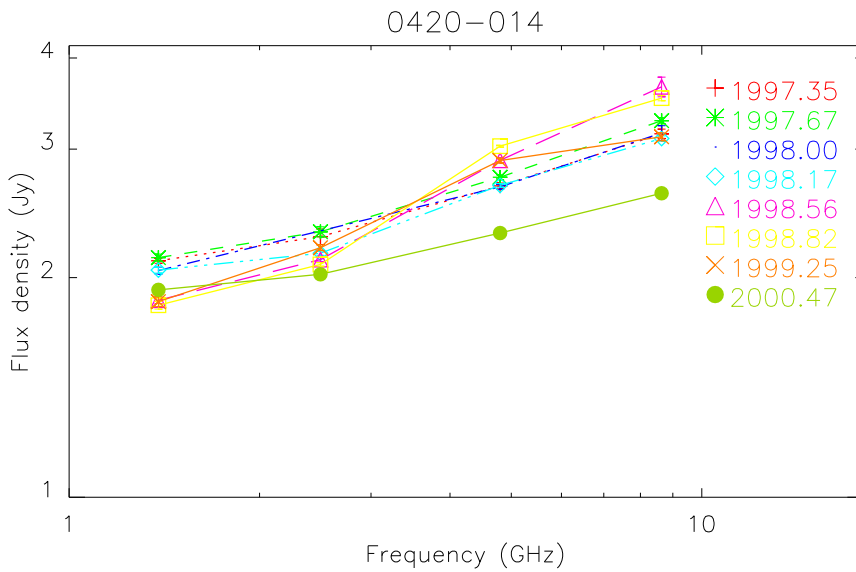
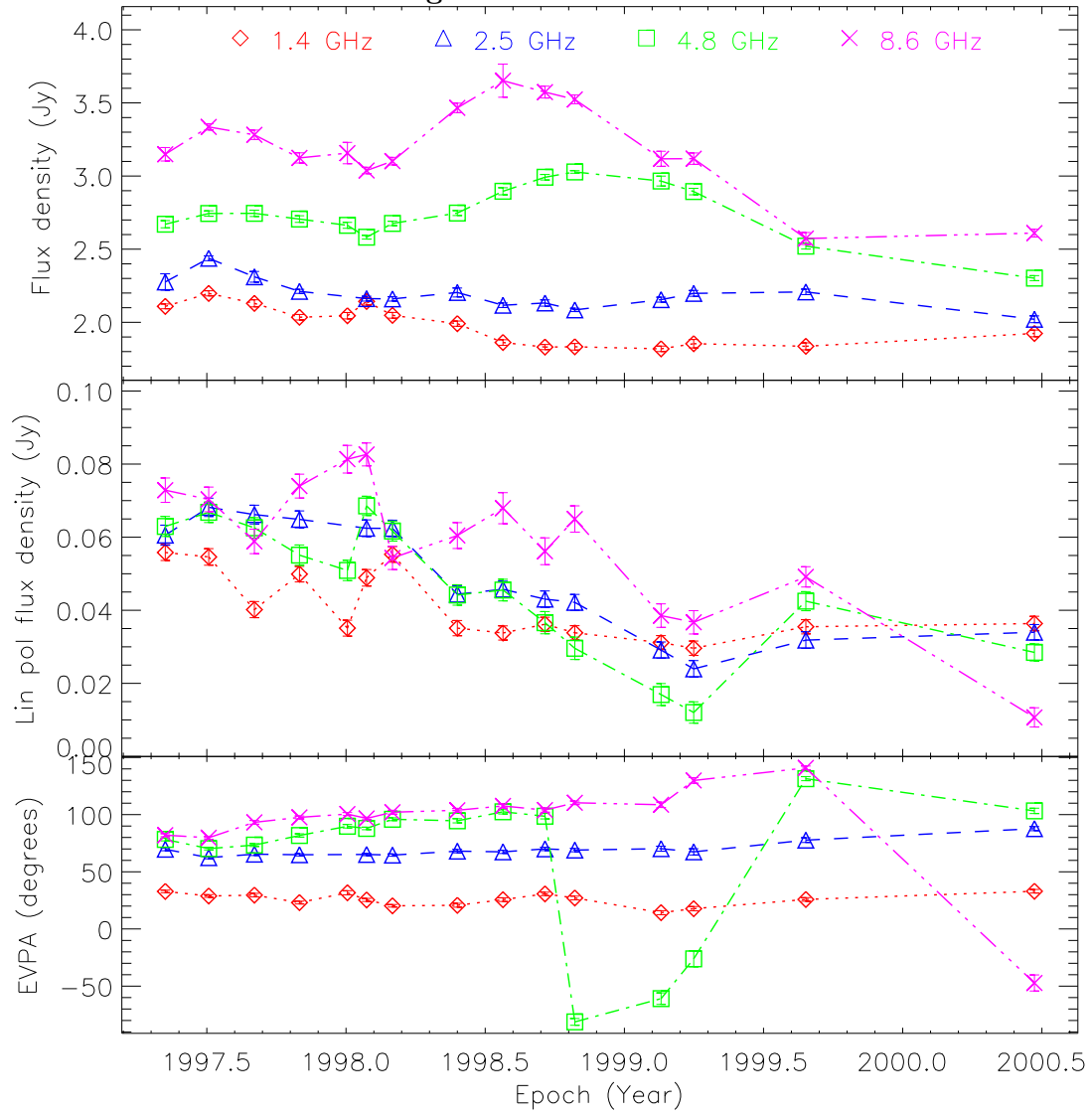


Figure A.4: PKS 0420-014



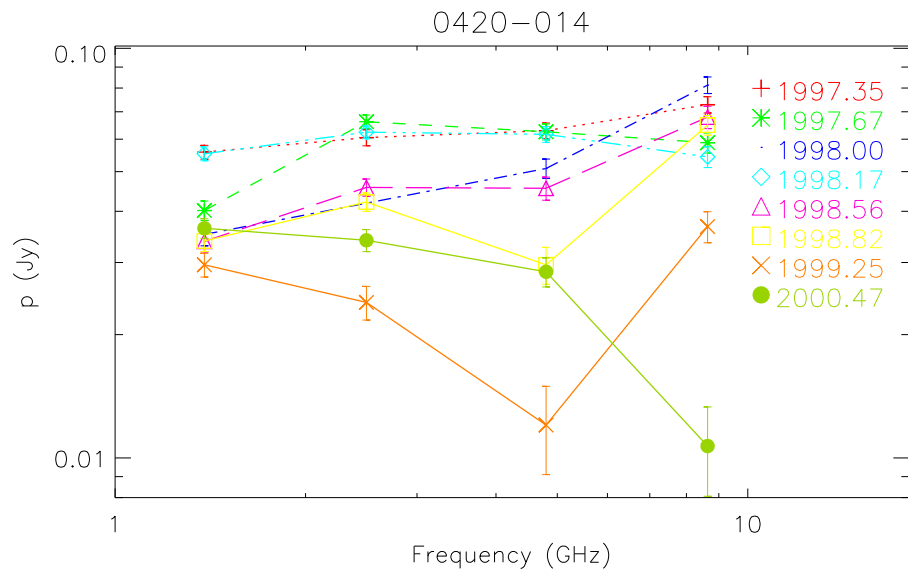
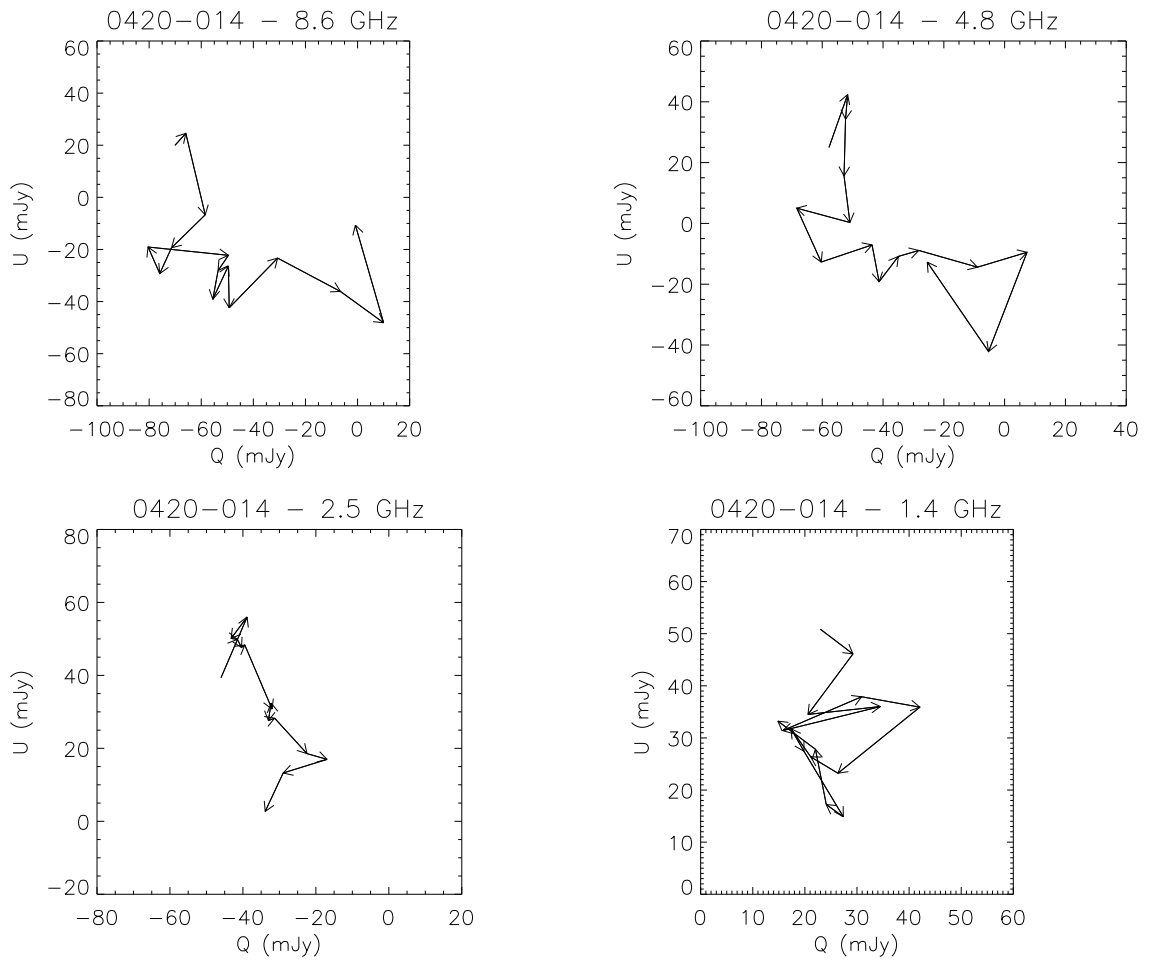
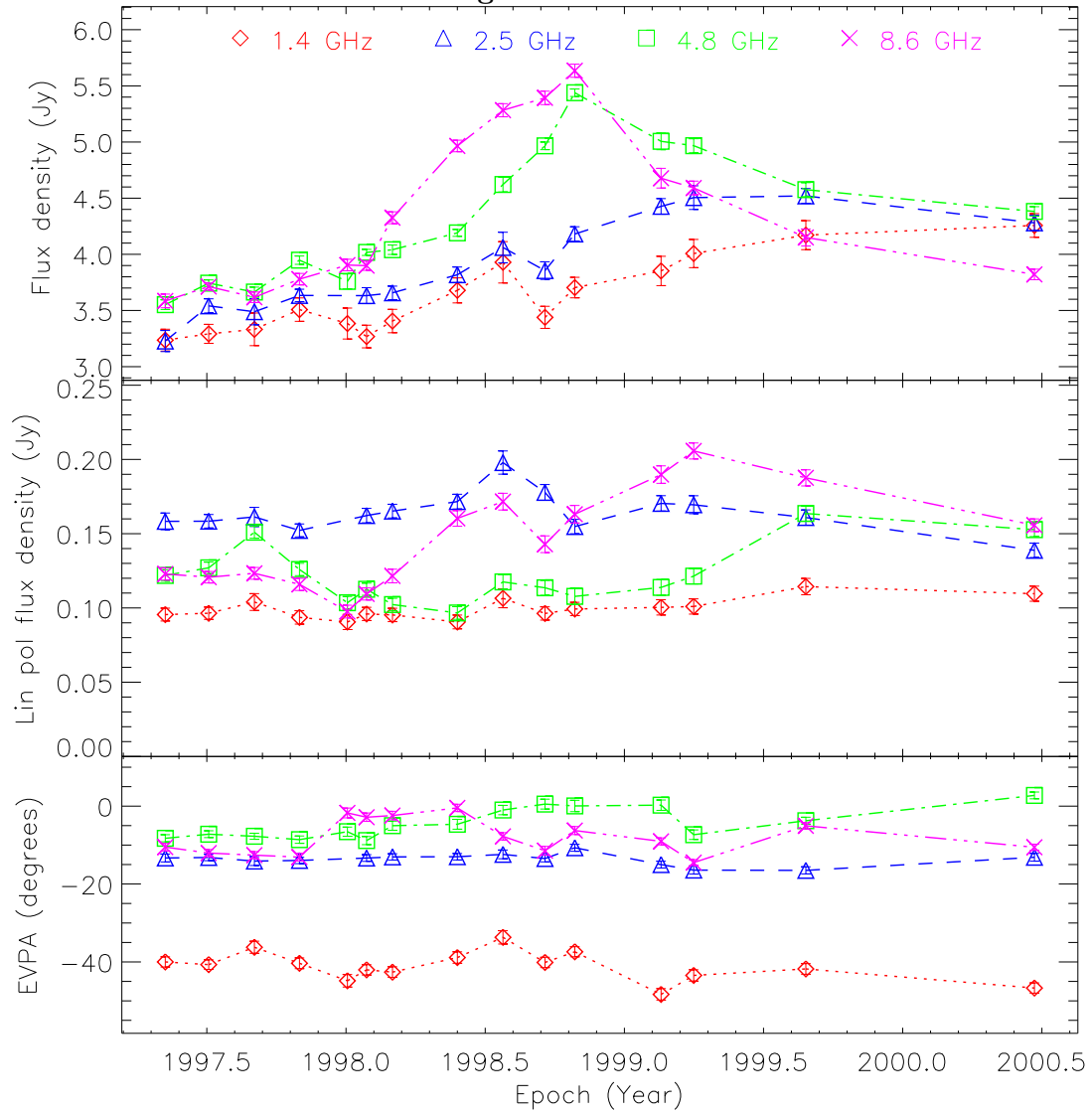
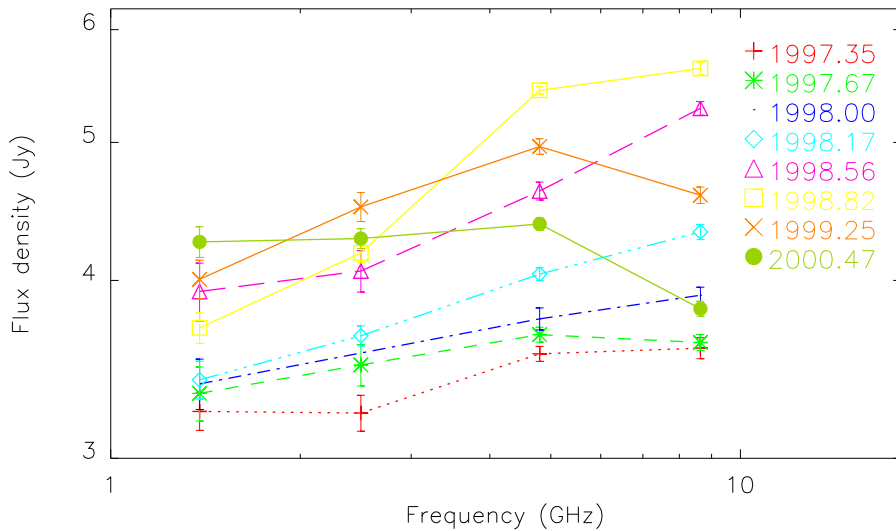


Figure A.5: 3C 120



0430+052



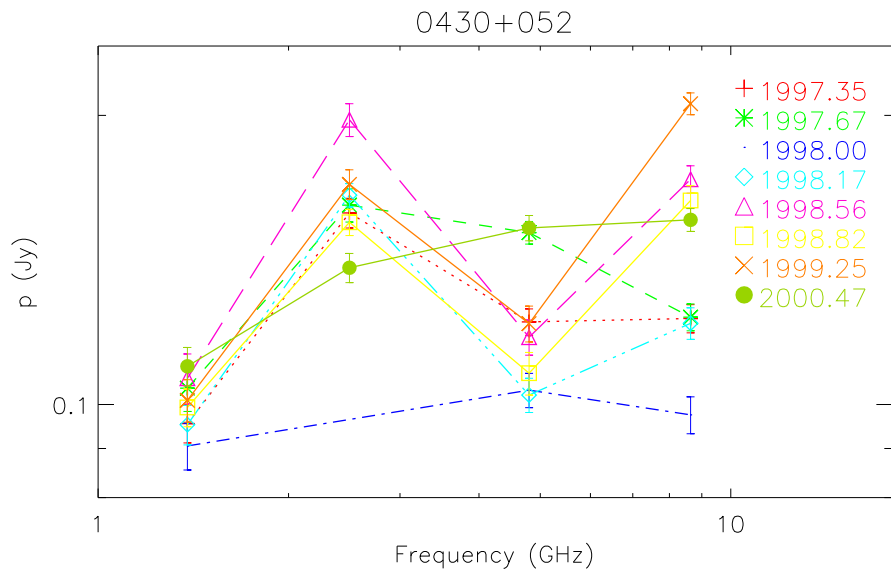
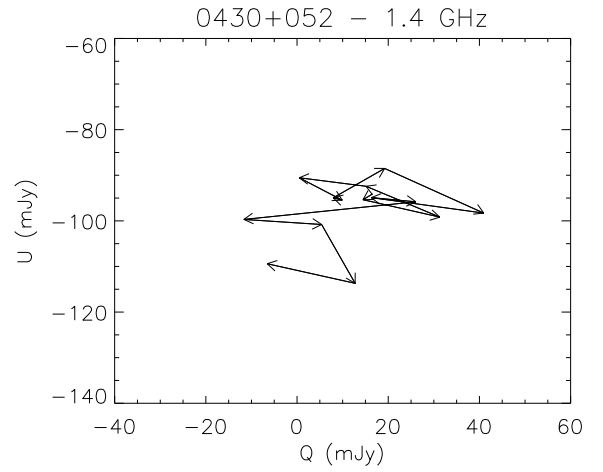
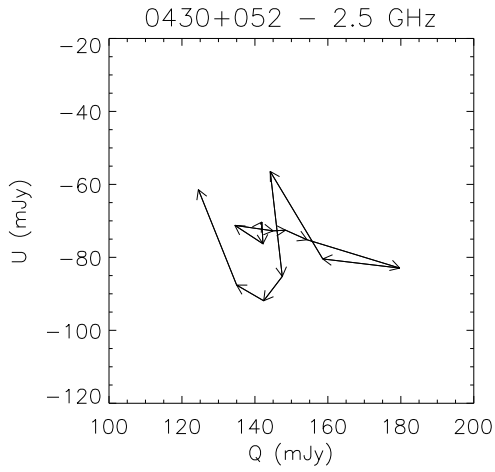
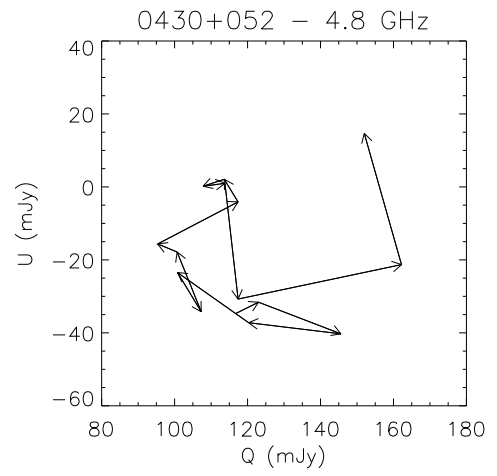
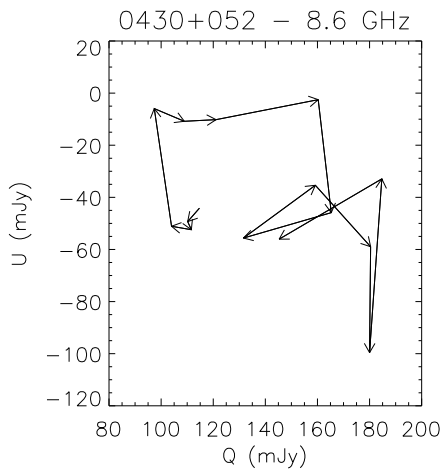
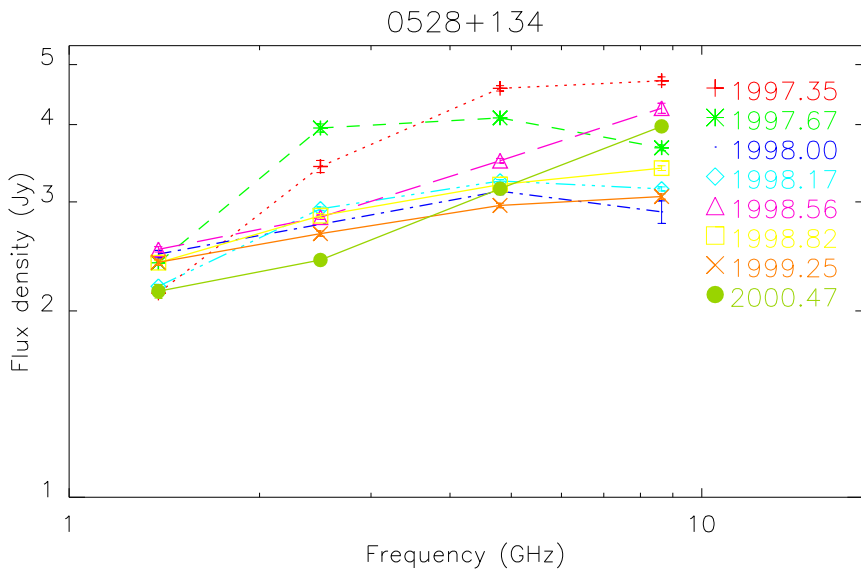
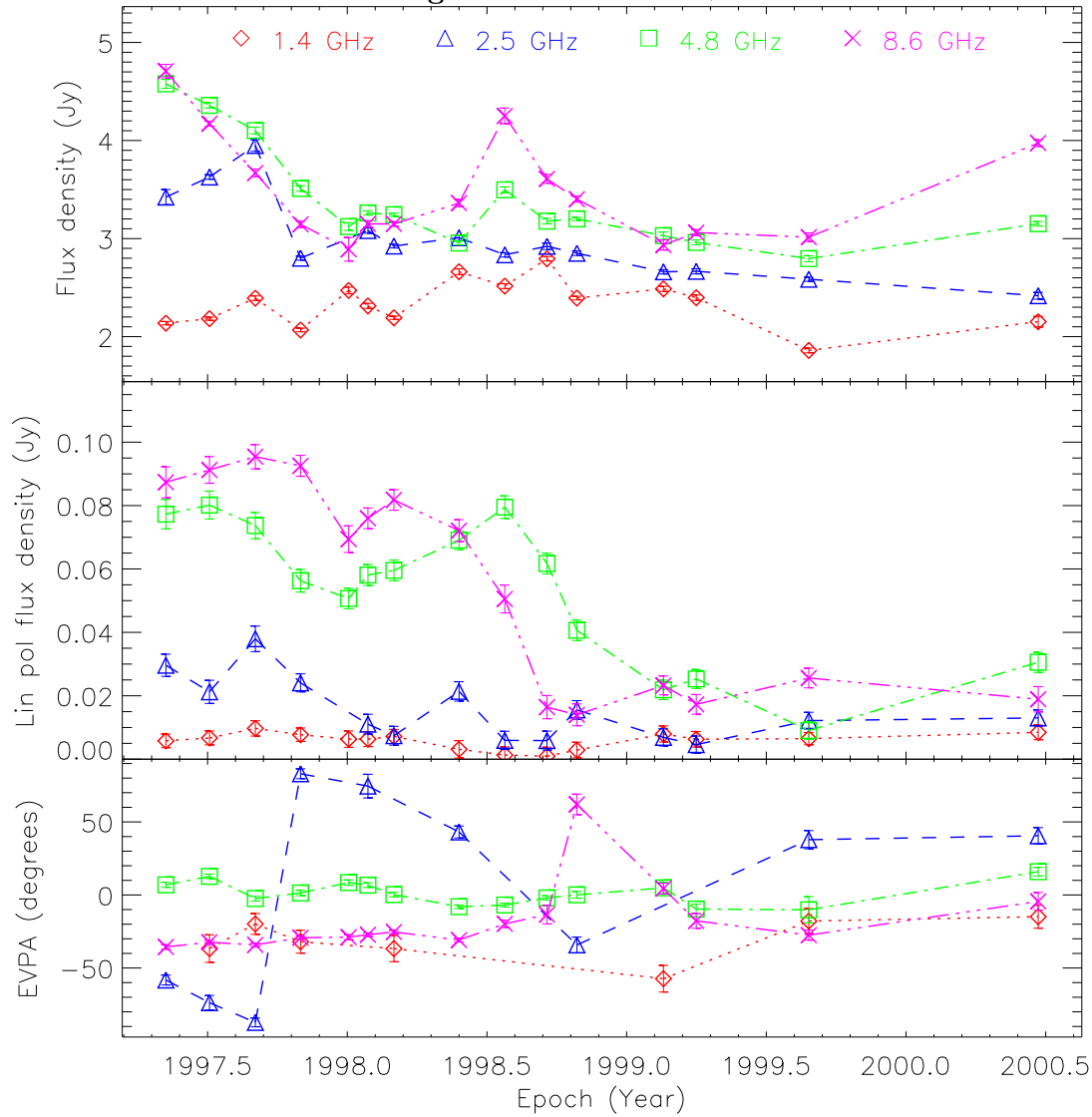


Figure A.6: PKS 0528+134



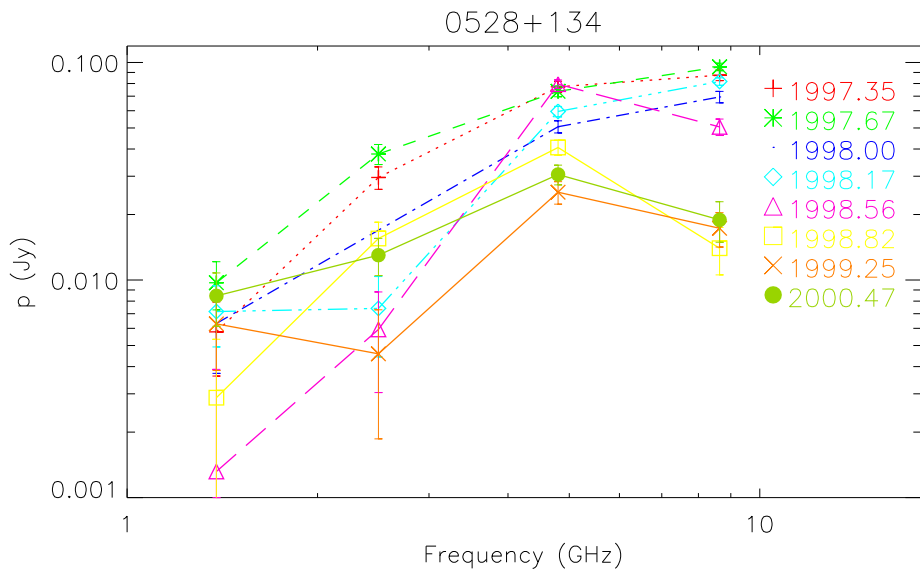
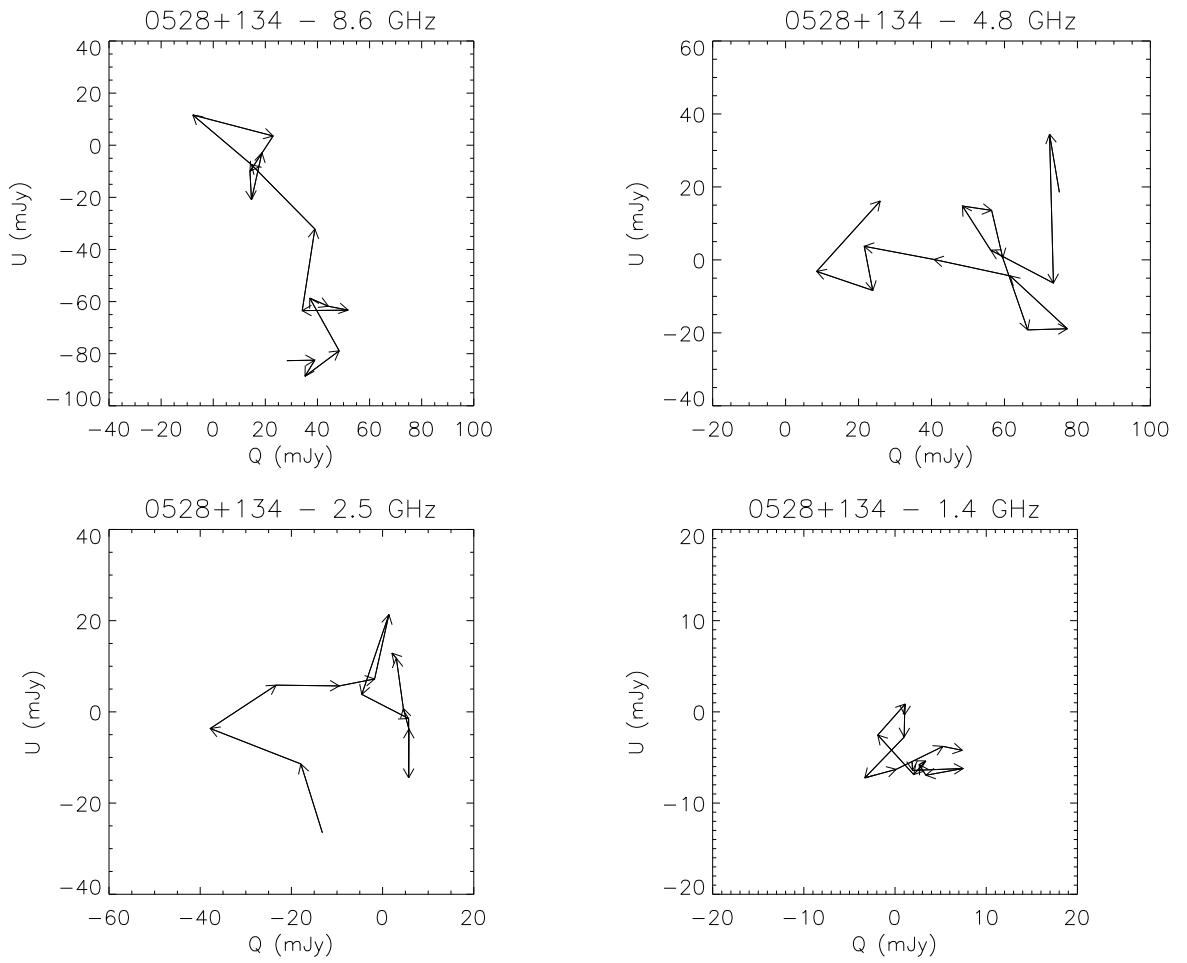
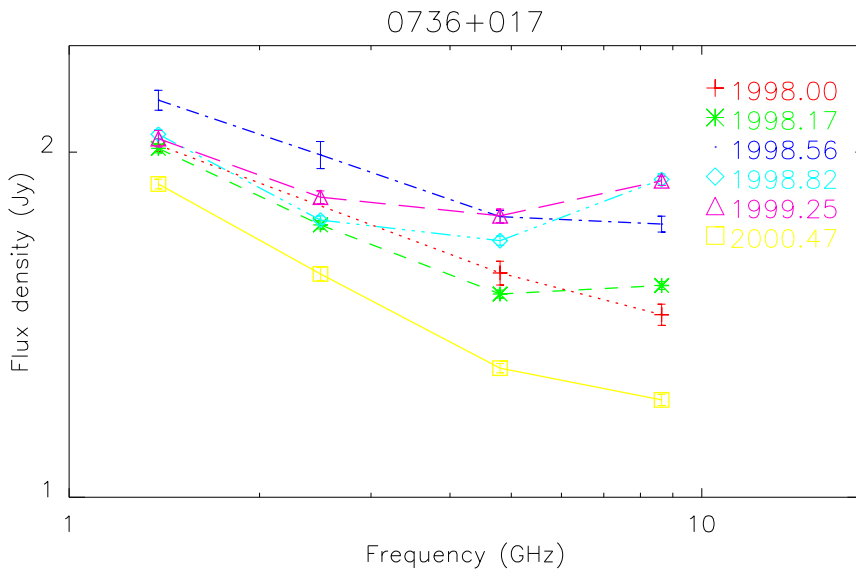
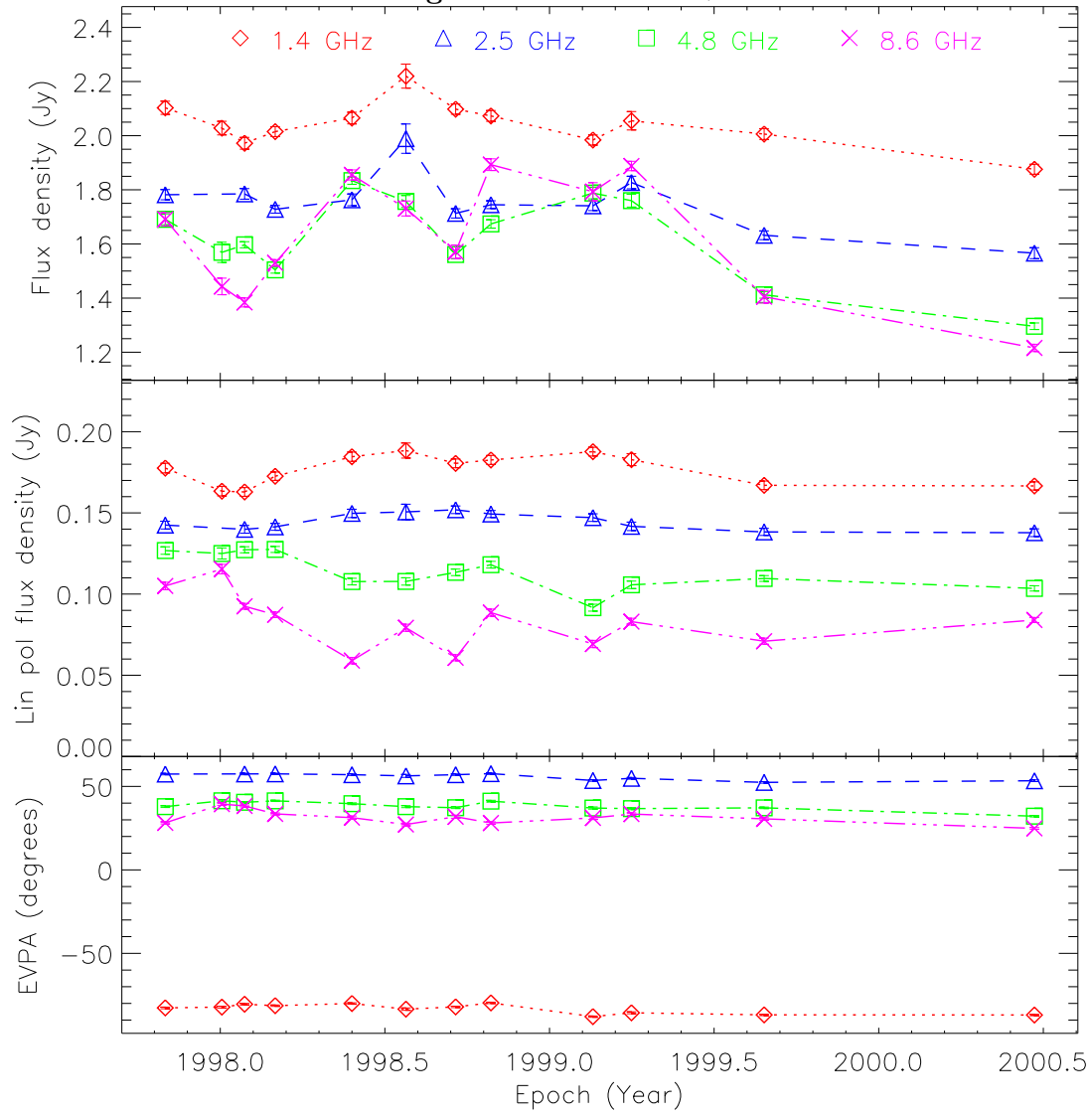


Figure A.7: PKS 0736+017



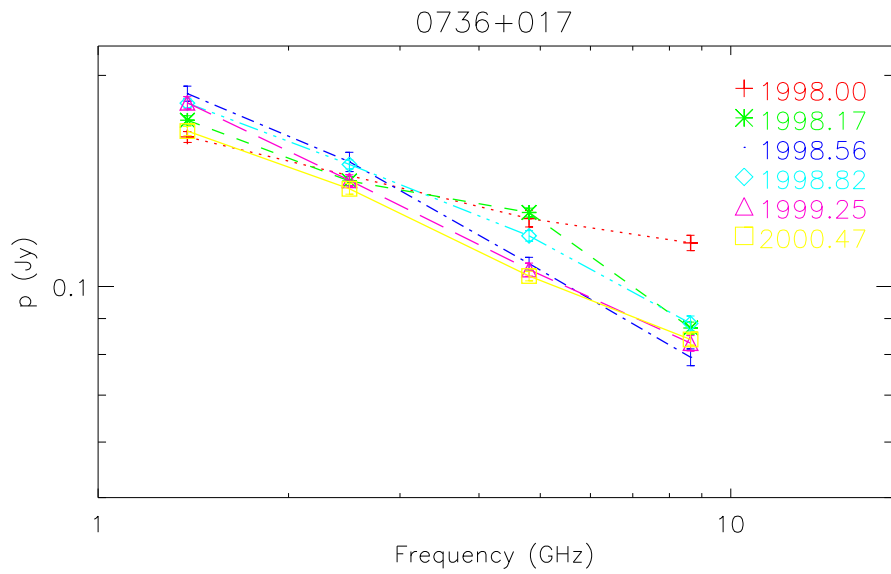
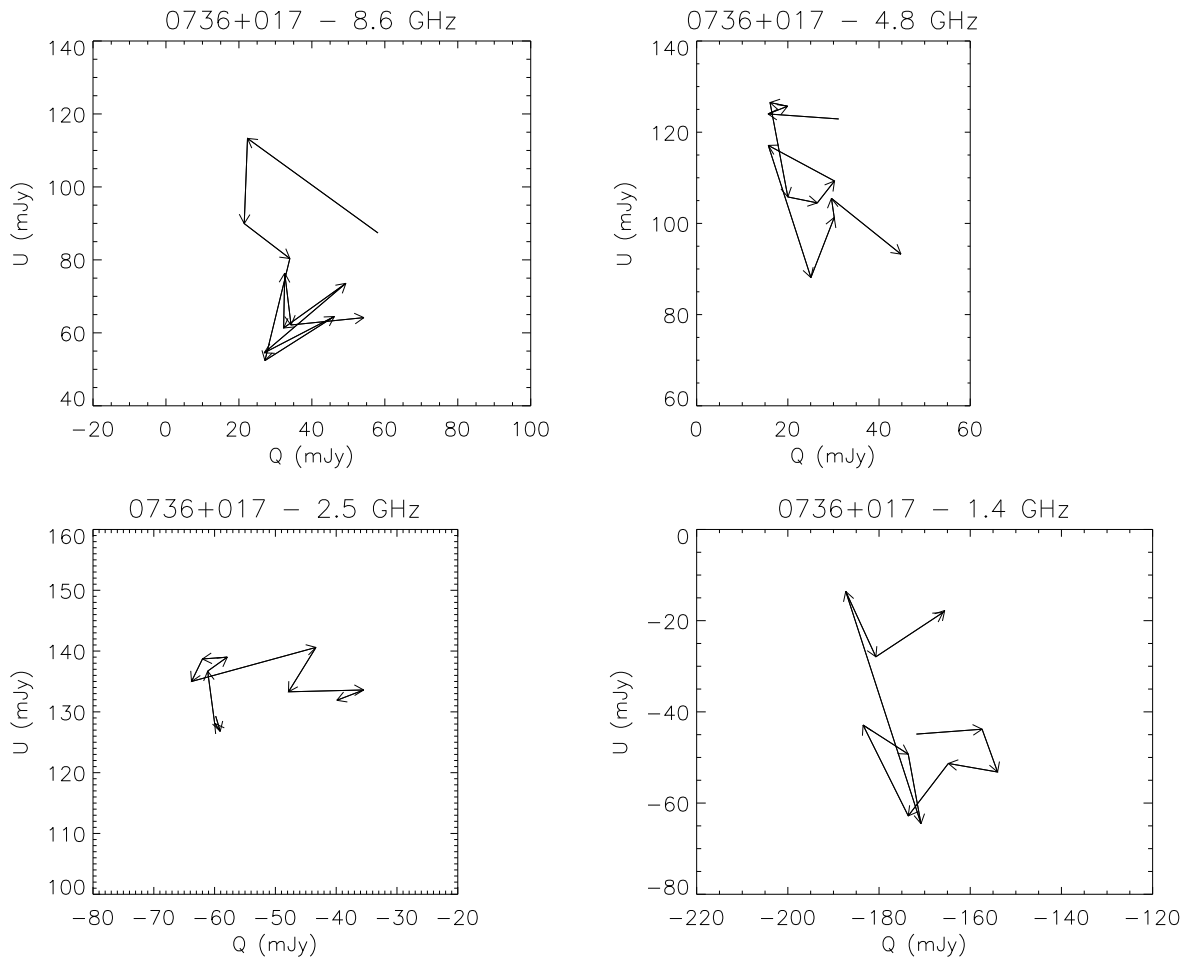
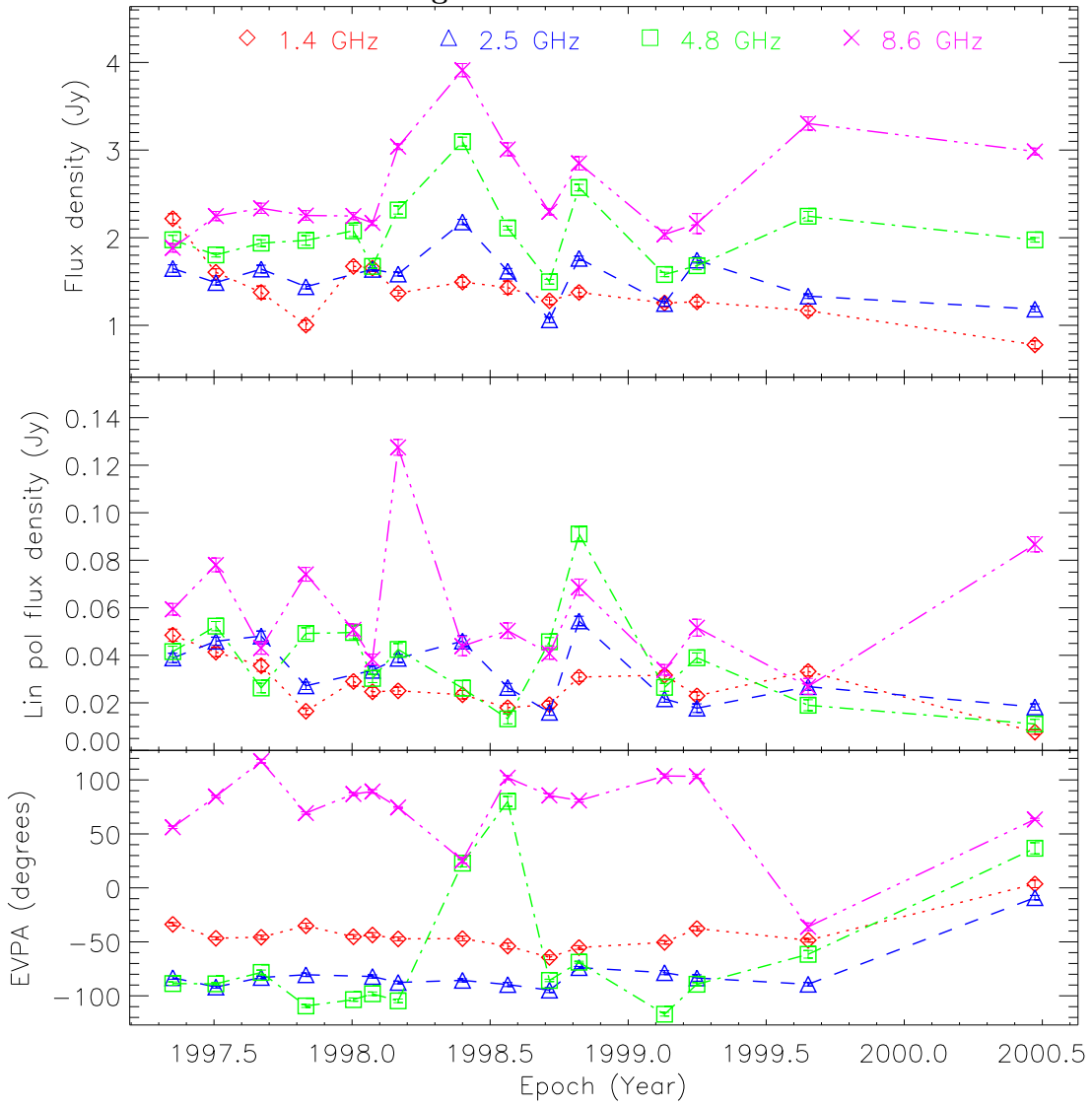
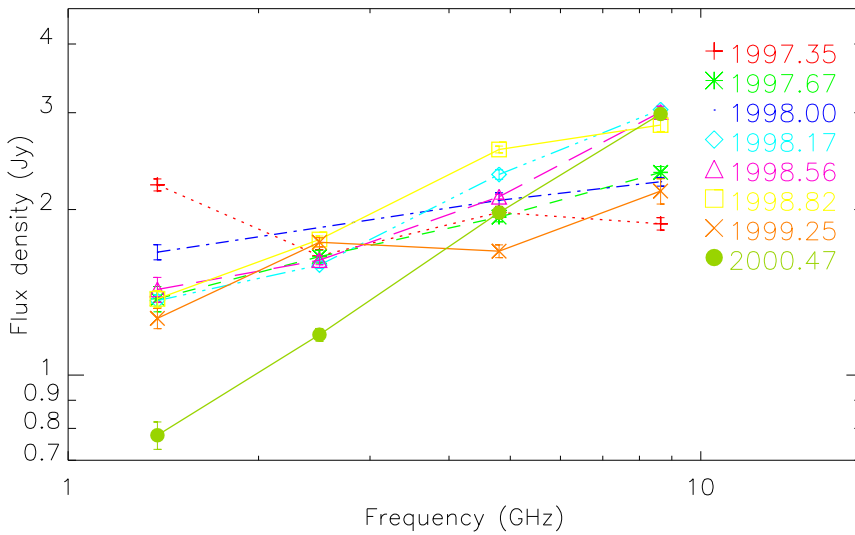


Figure A.8: PKS 1144–379



1144–379



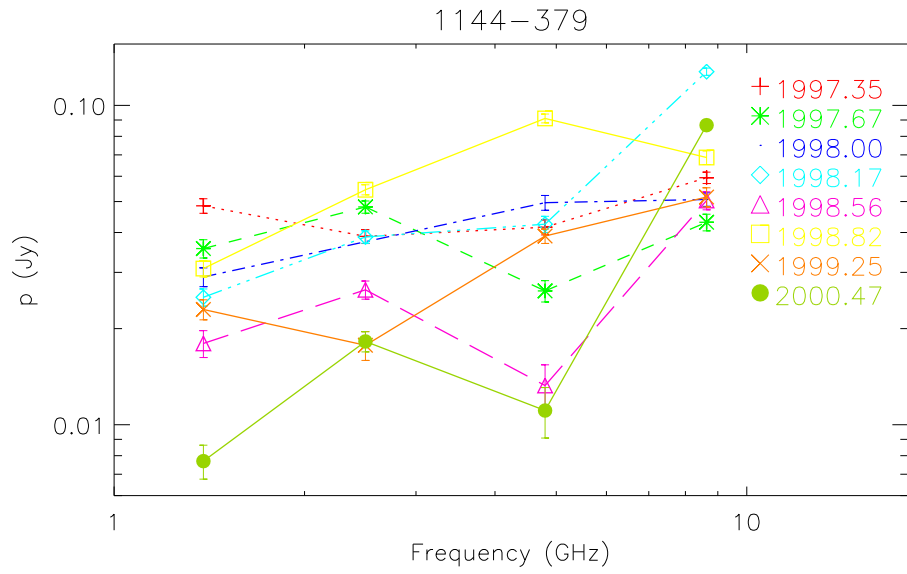
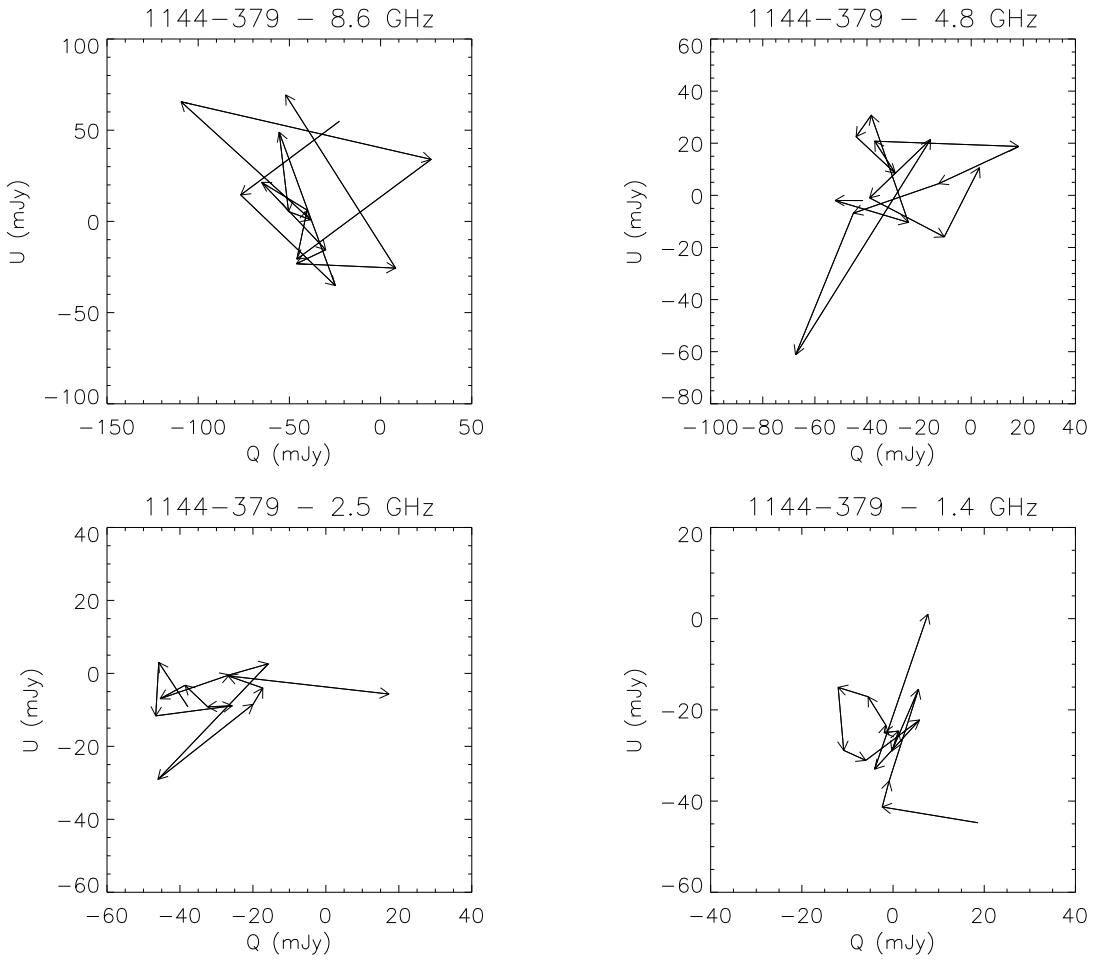
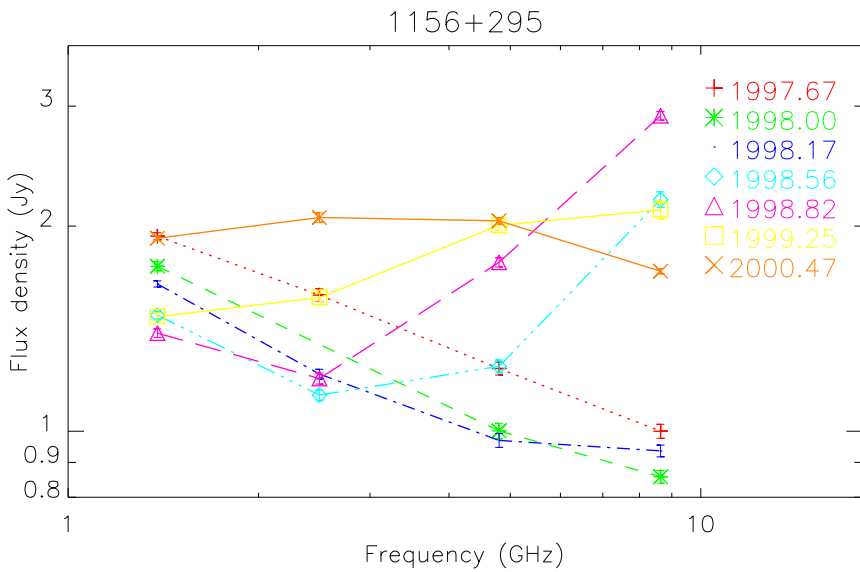
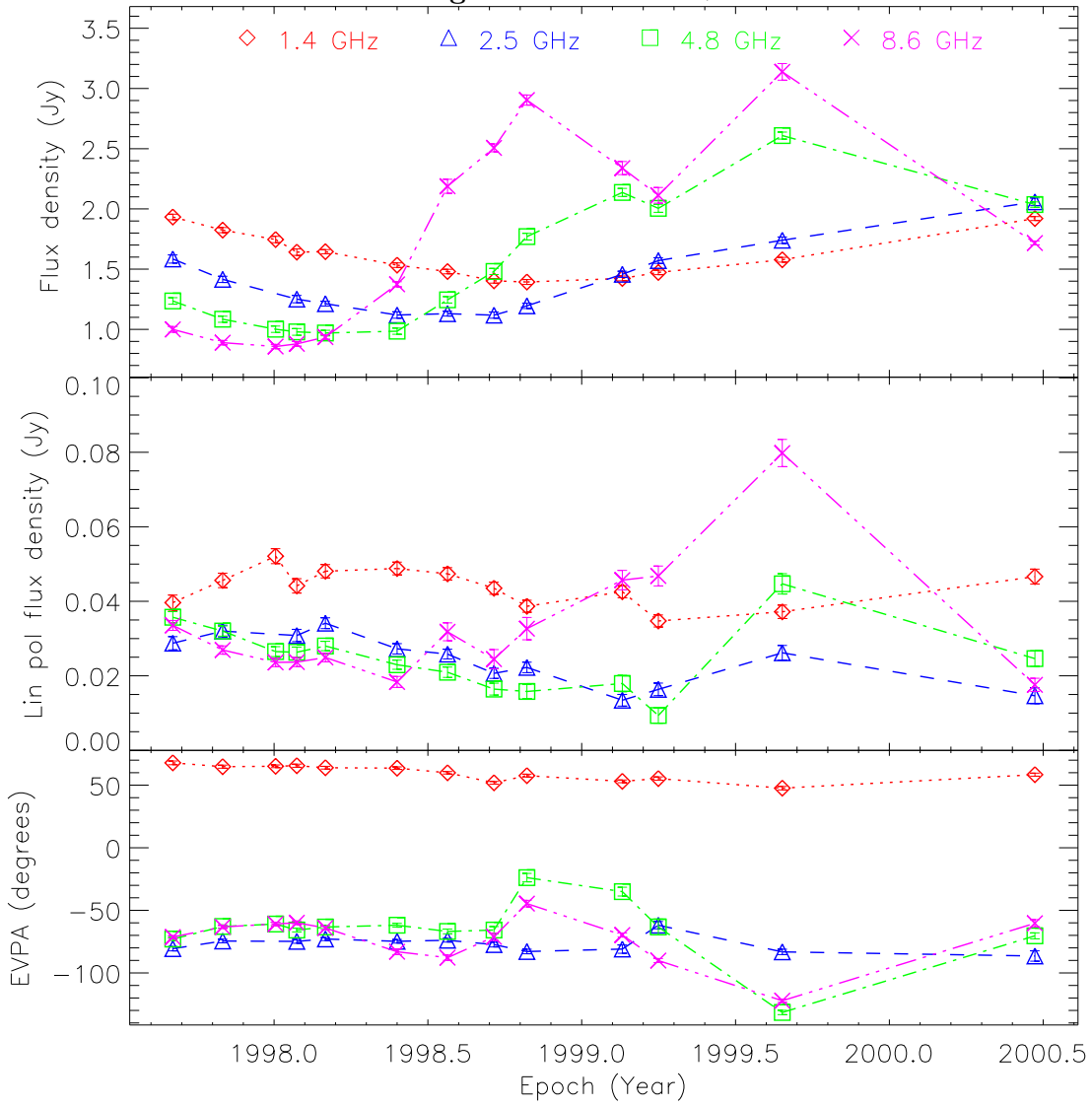


Figure A.9: B2 1156+29



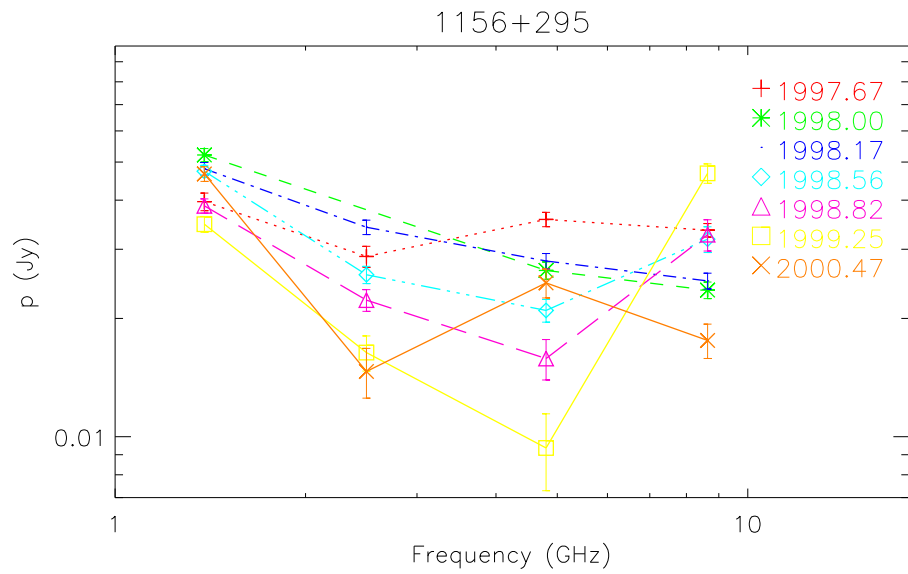
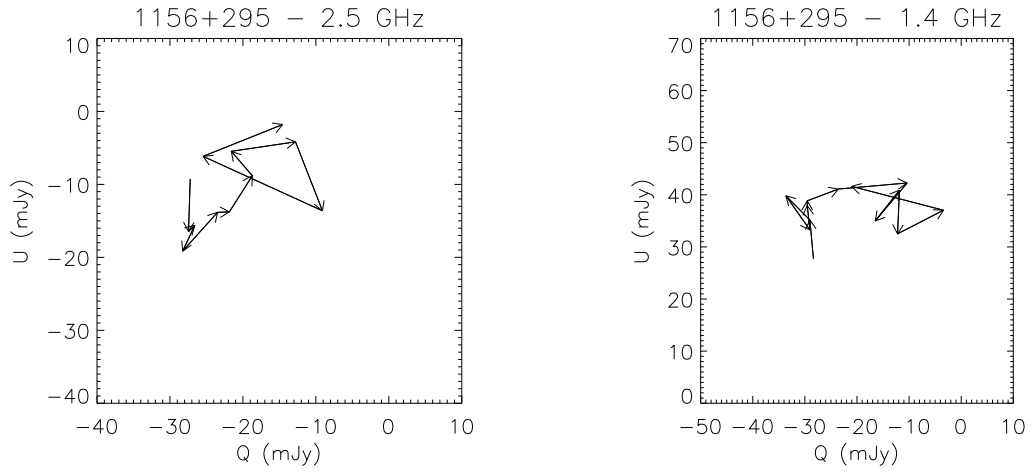
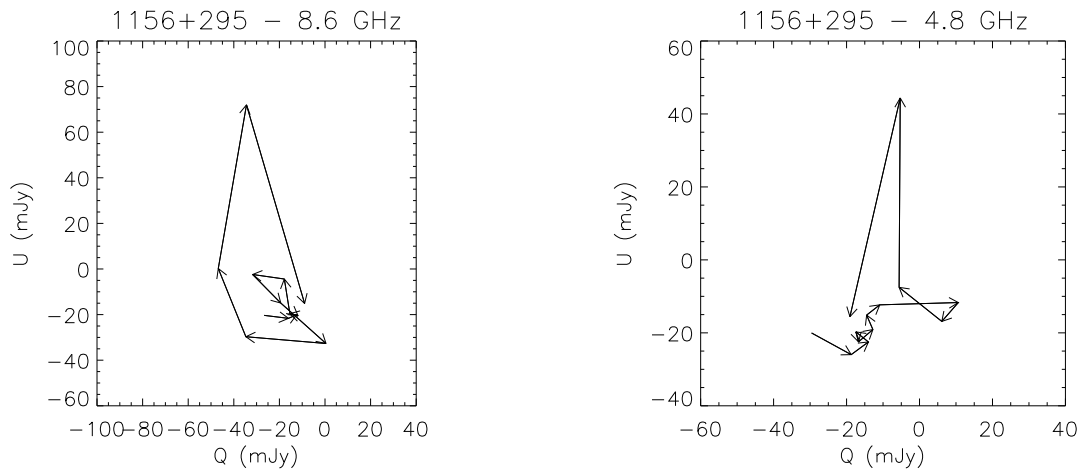
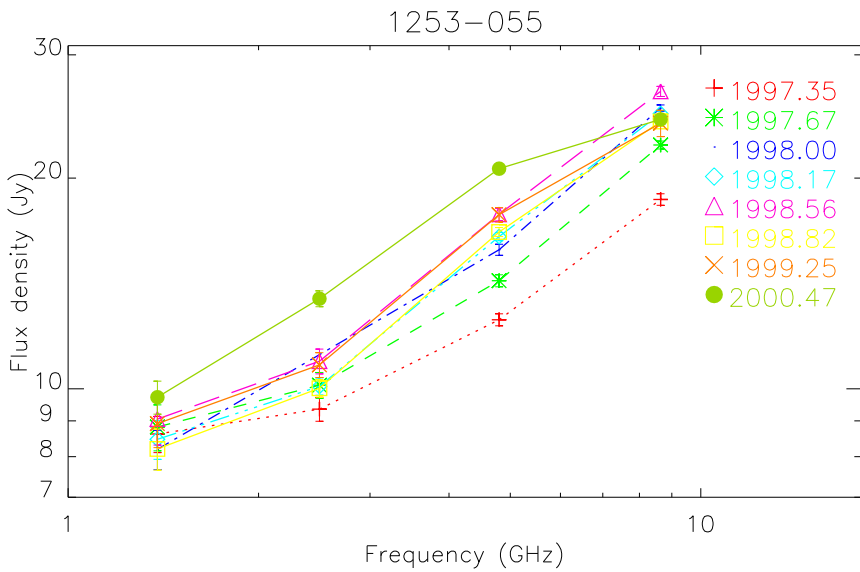
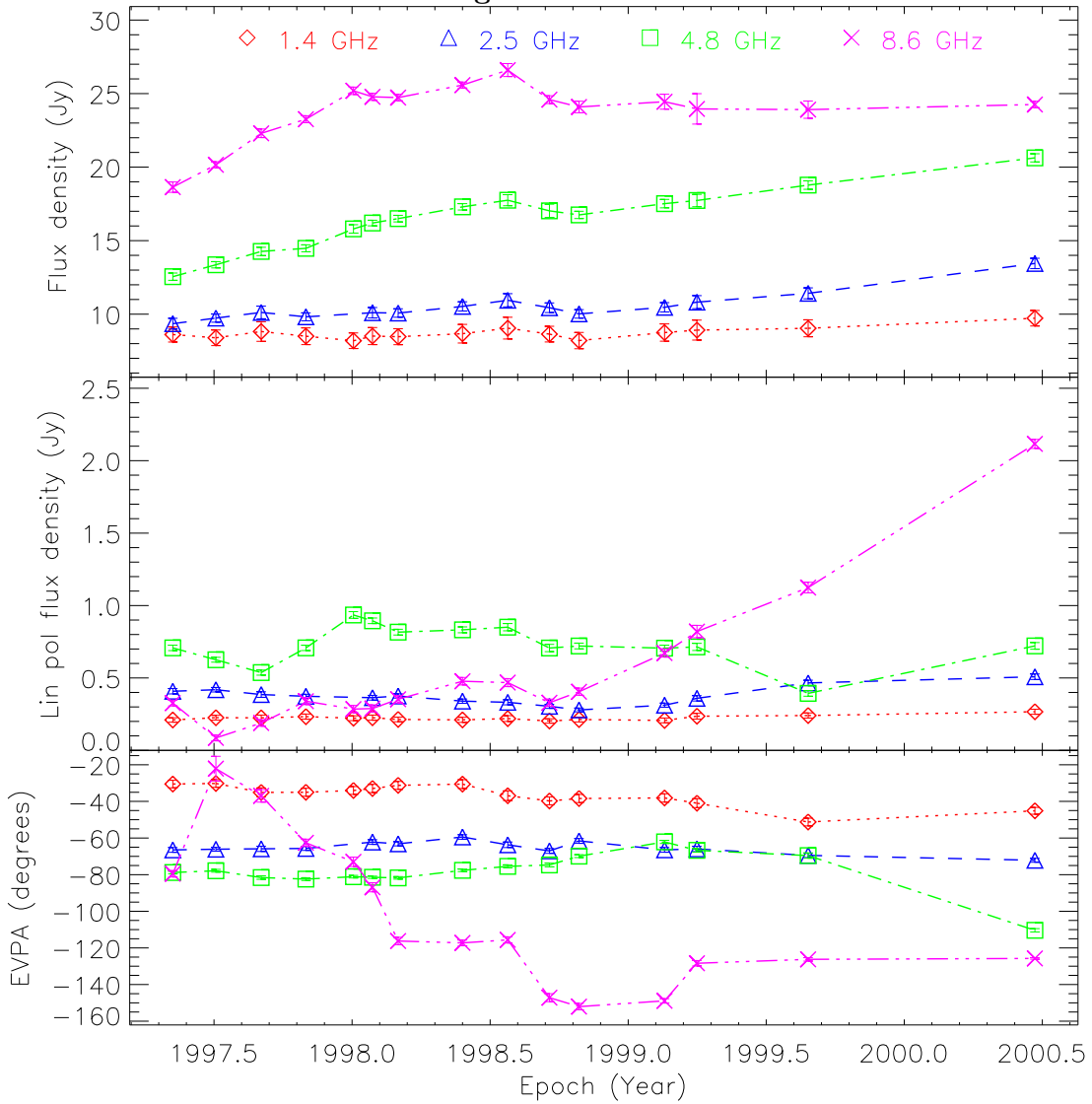


Figure A.10: 3C 279



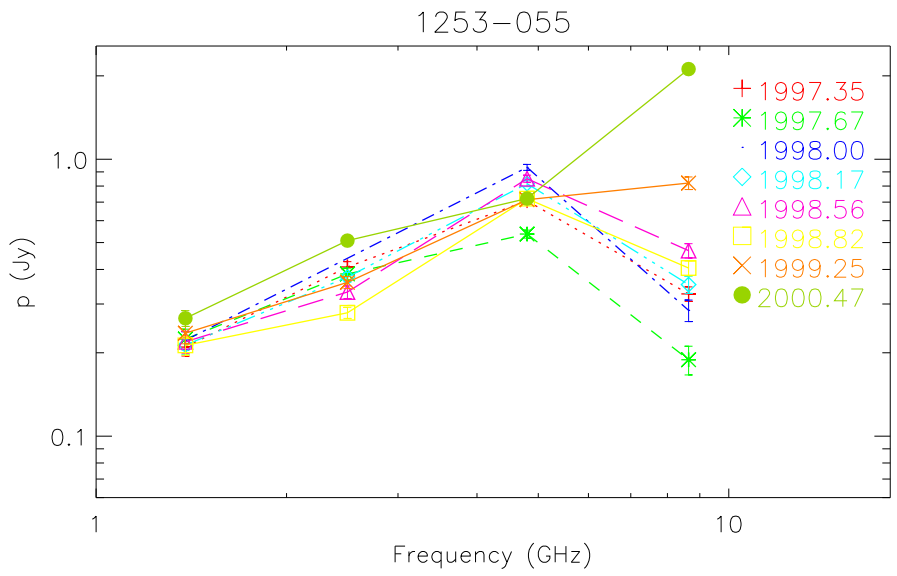
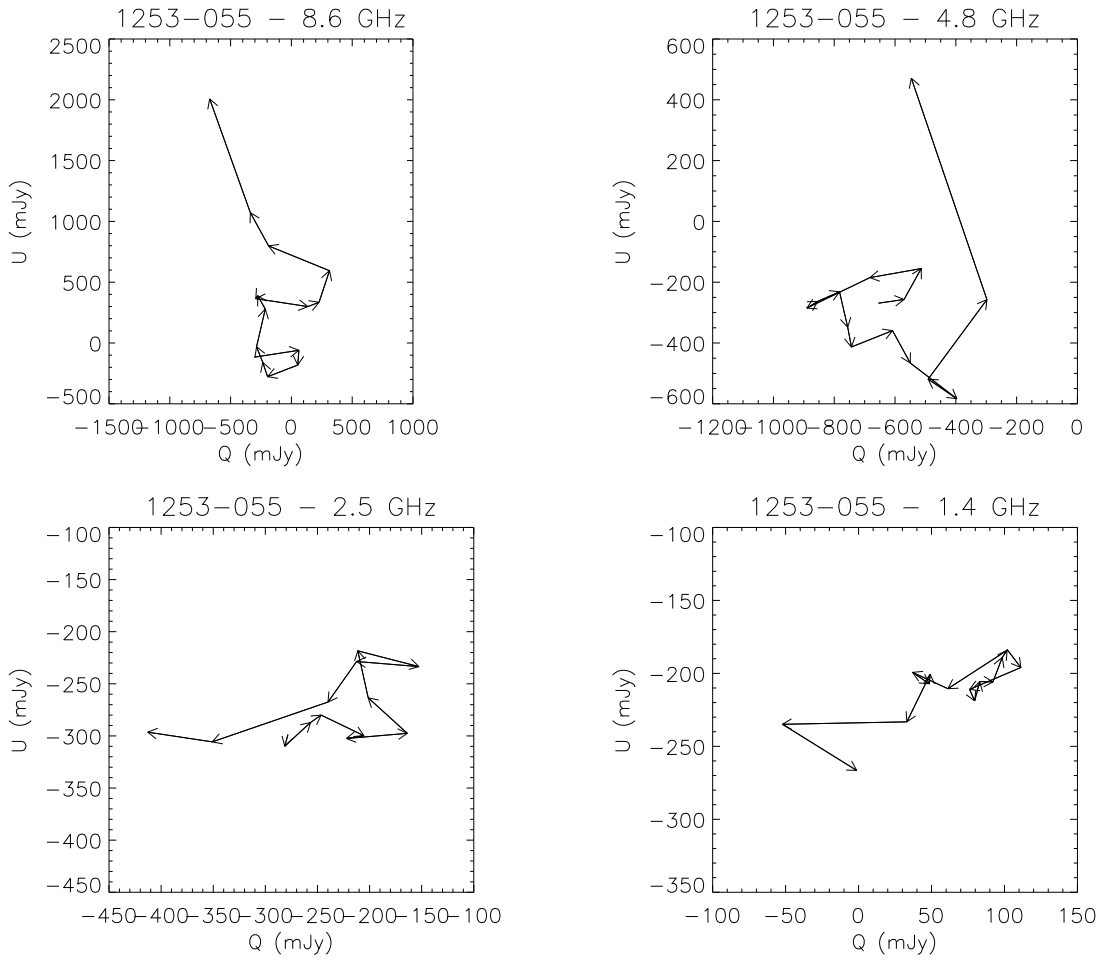
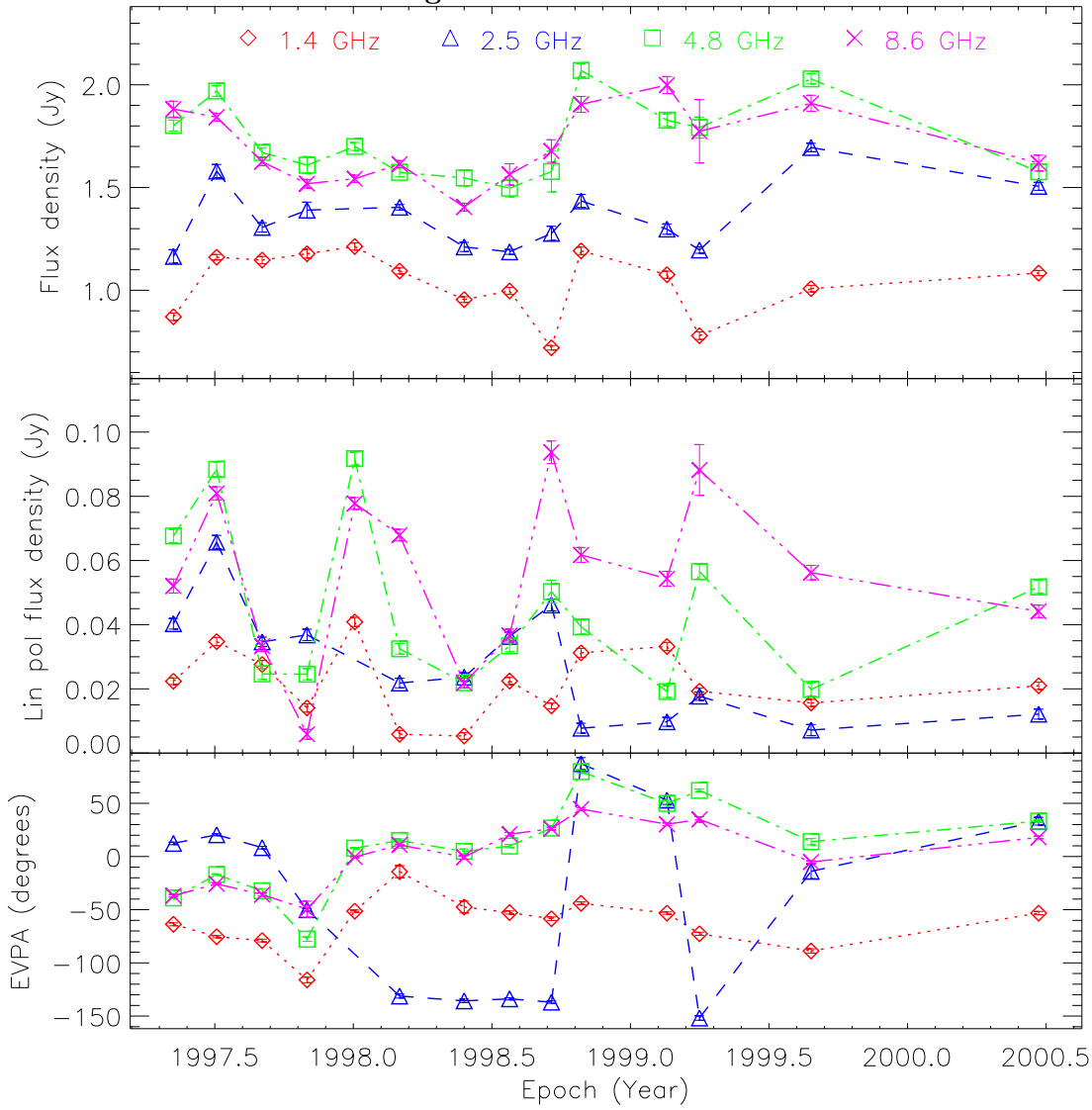
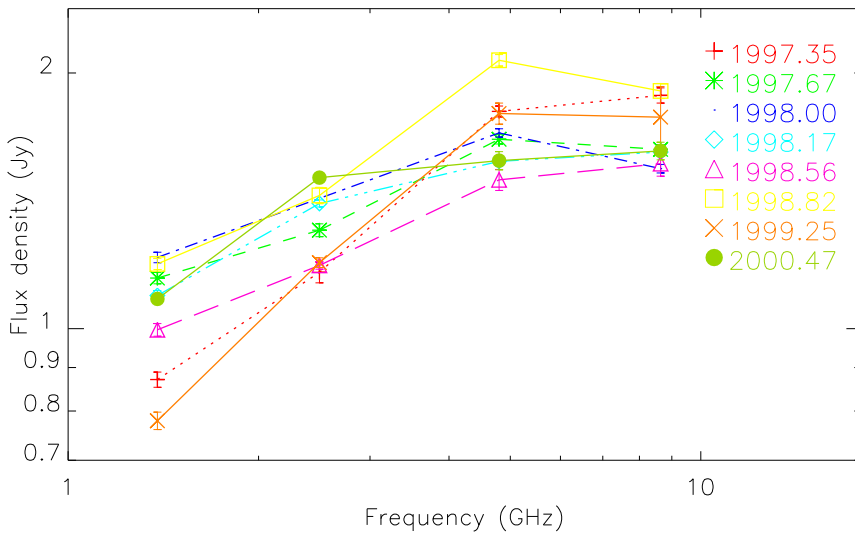


Figure A.11: PKS 1519–273



1519–273



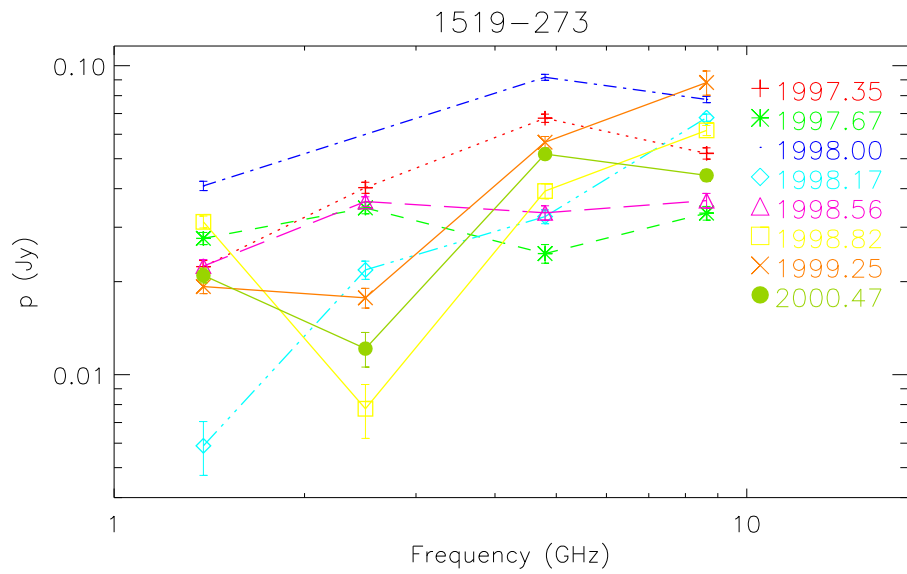
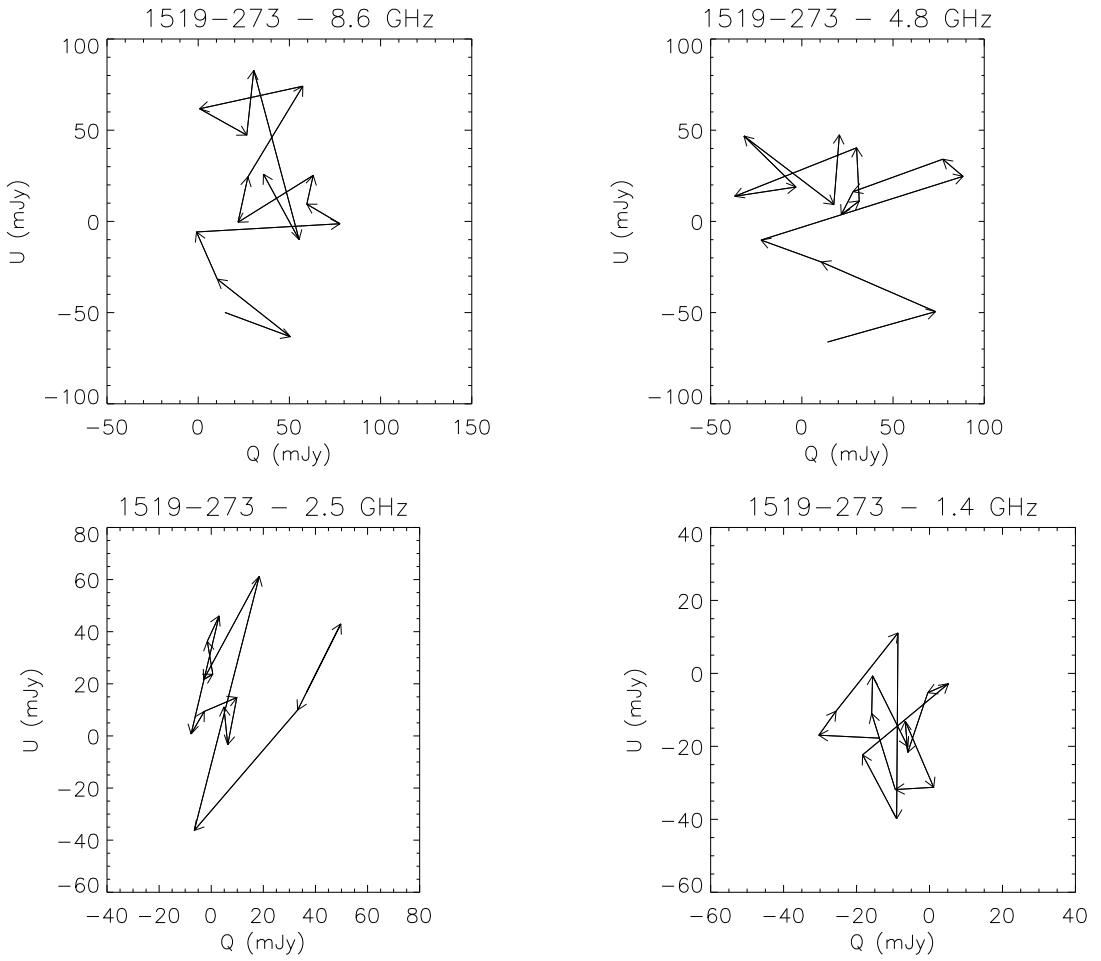
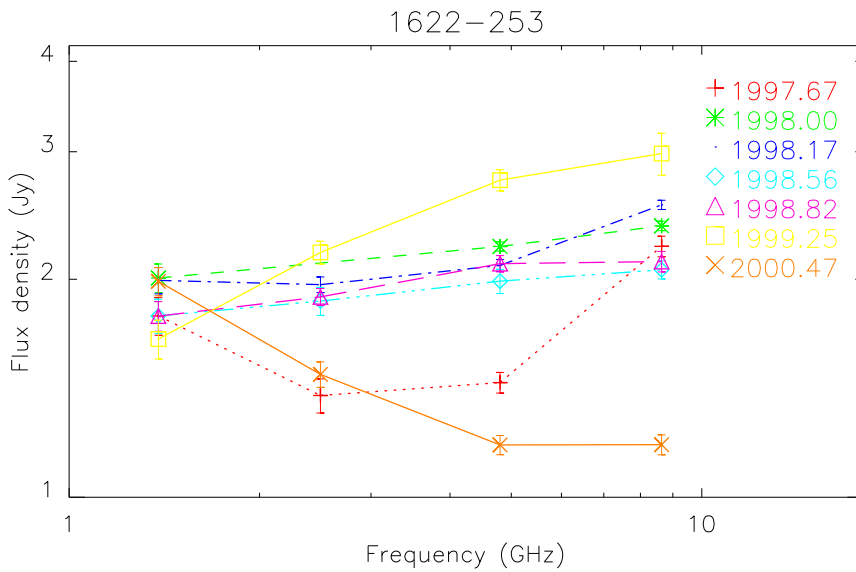
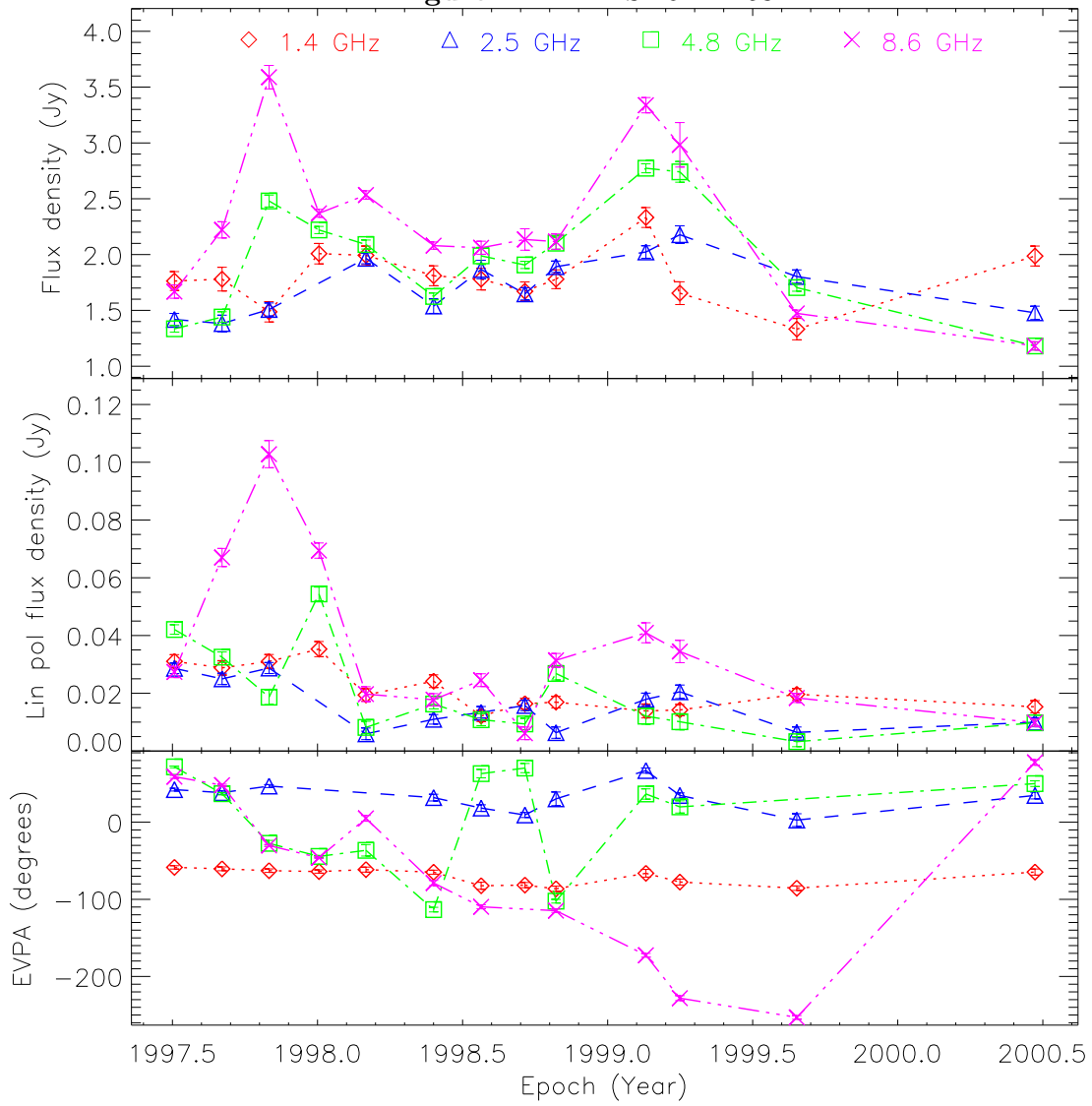


Figure A.12: PKS 1622–253



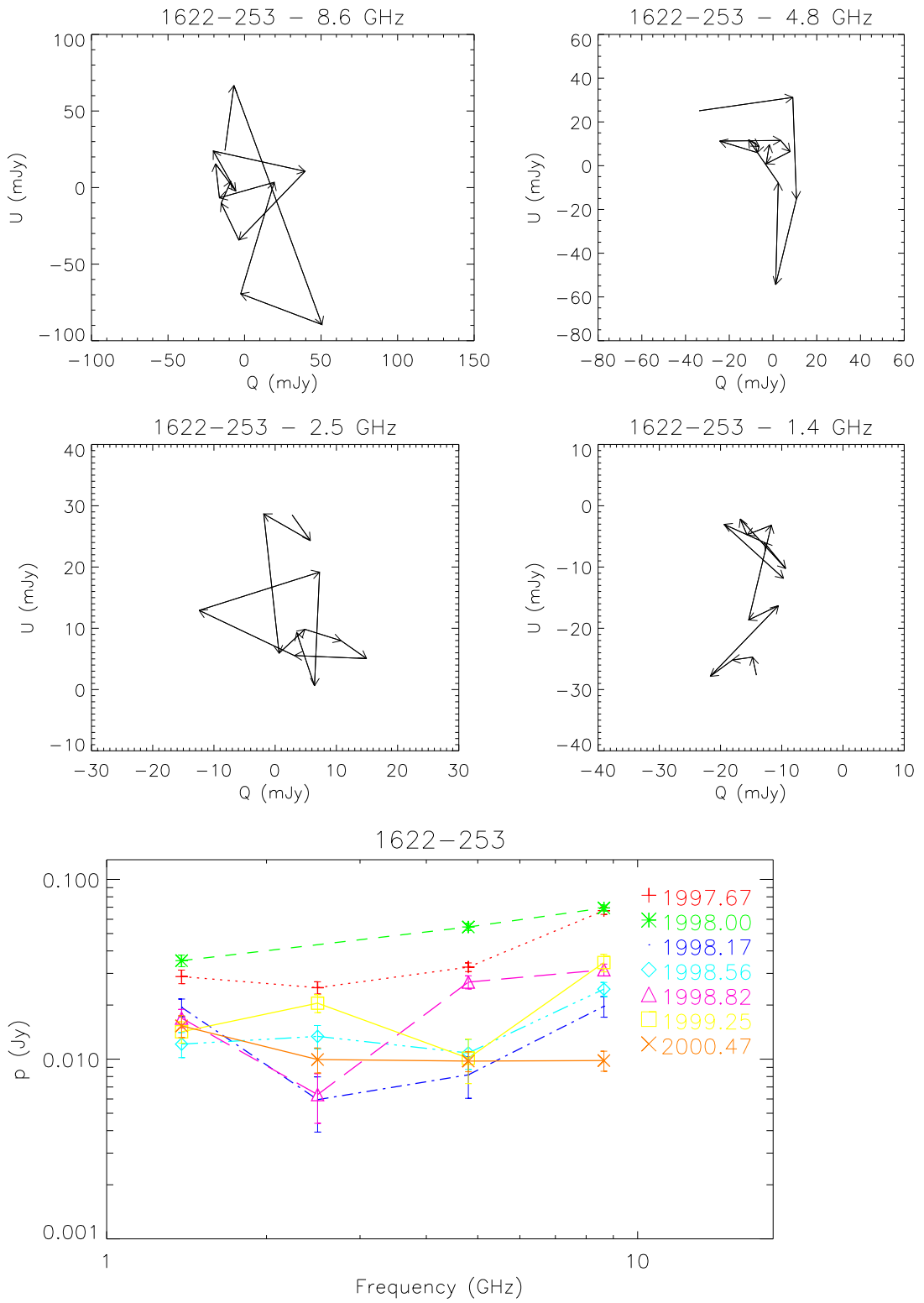


Figure A.13: NRAO 530

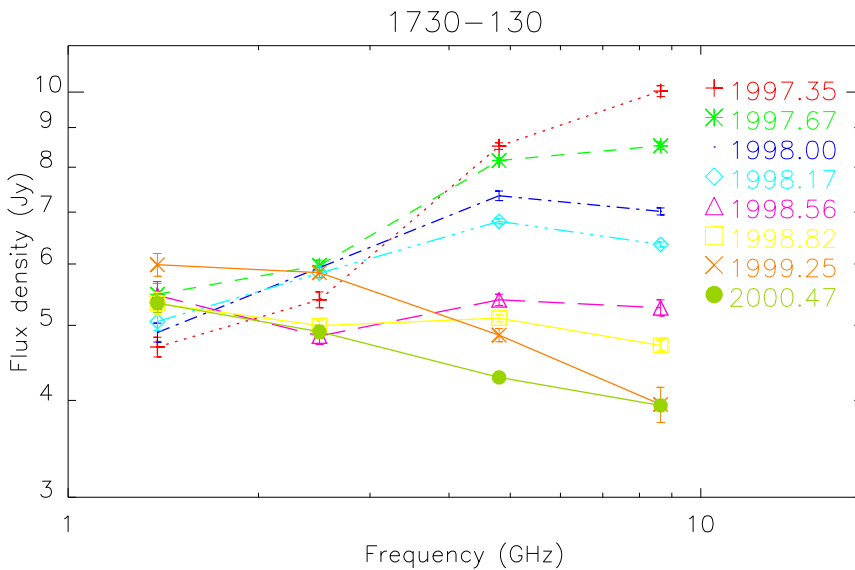
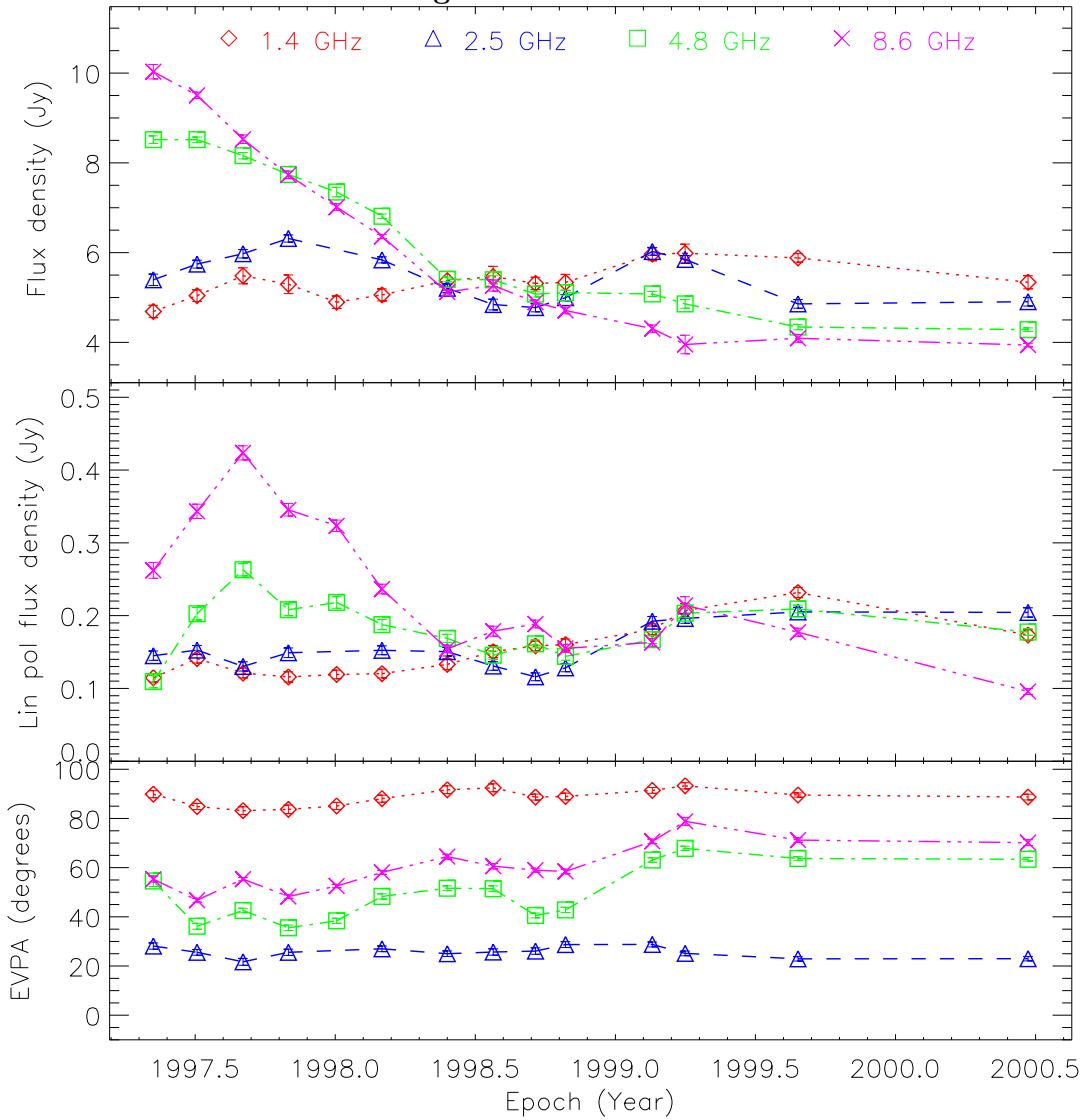
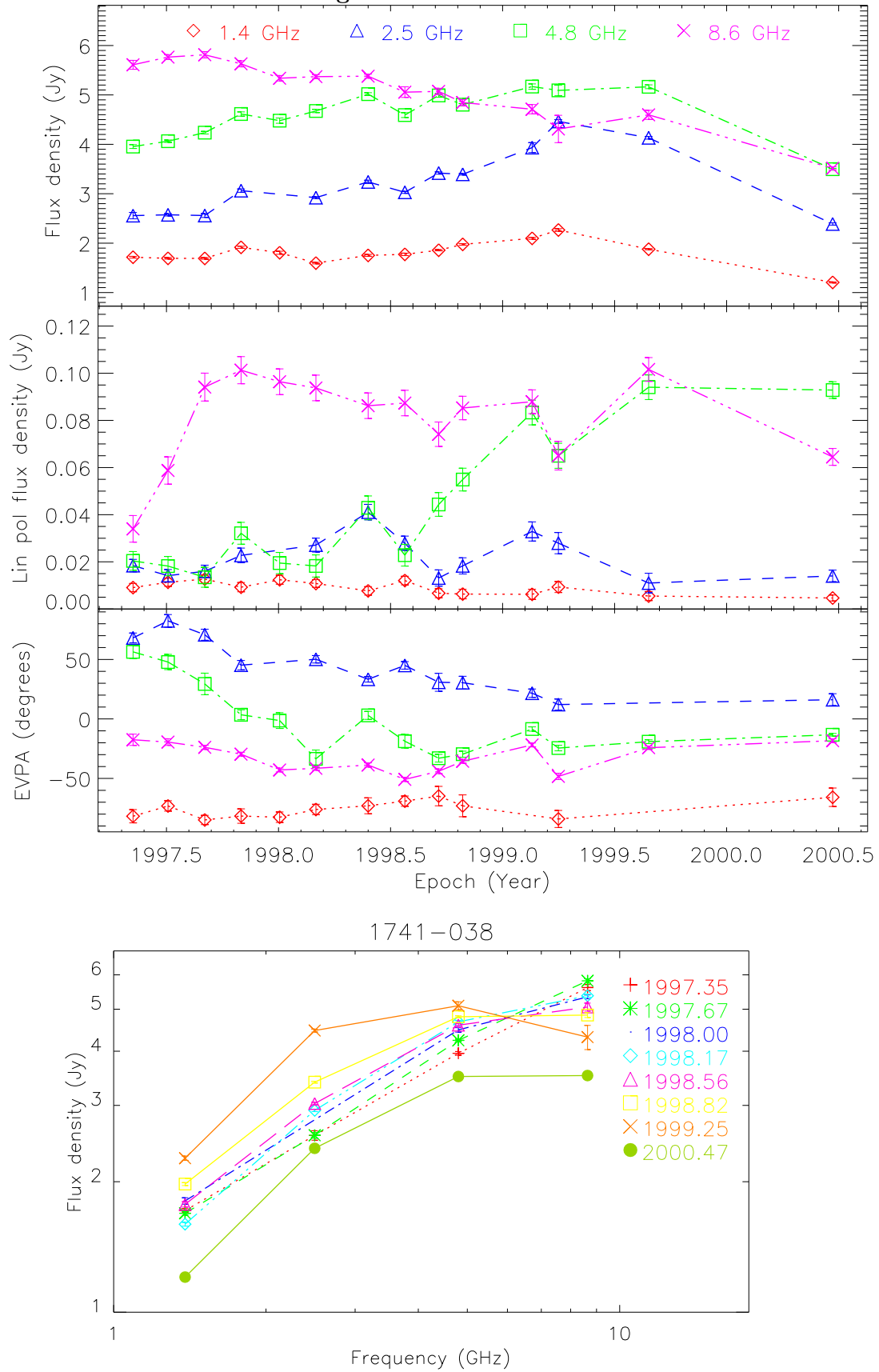


Figure A.14: PKS 1741-038



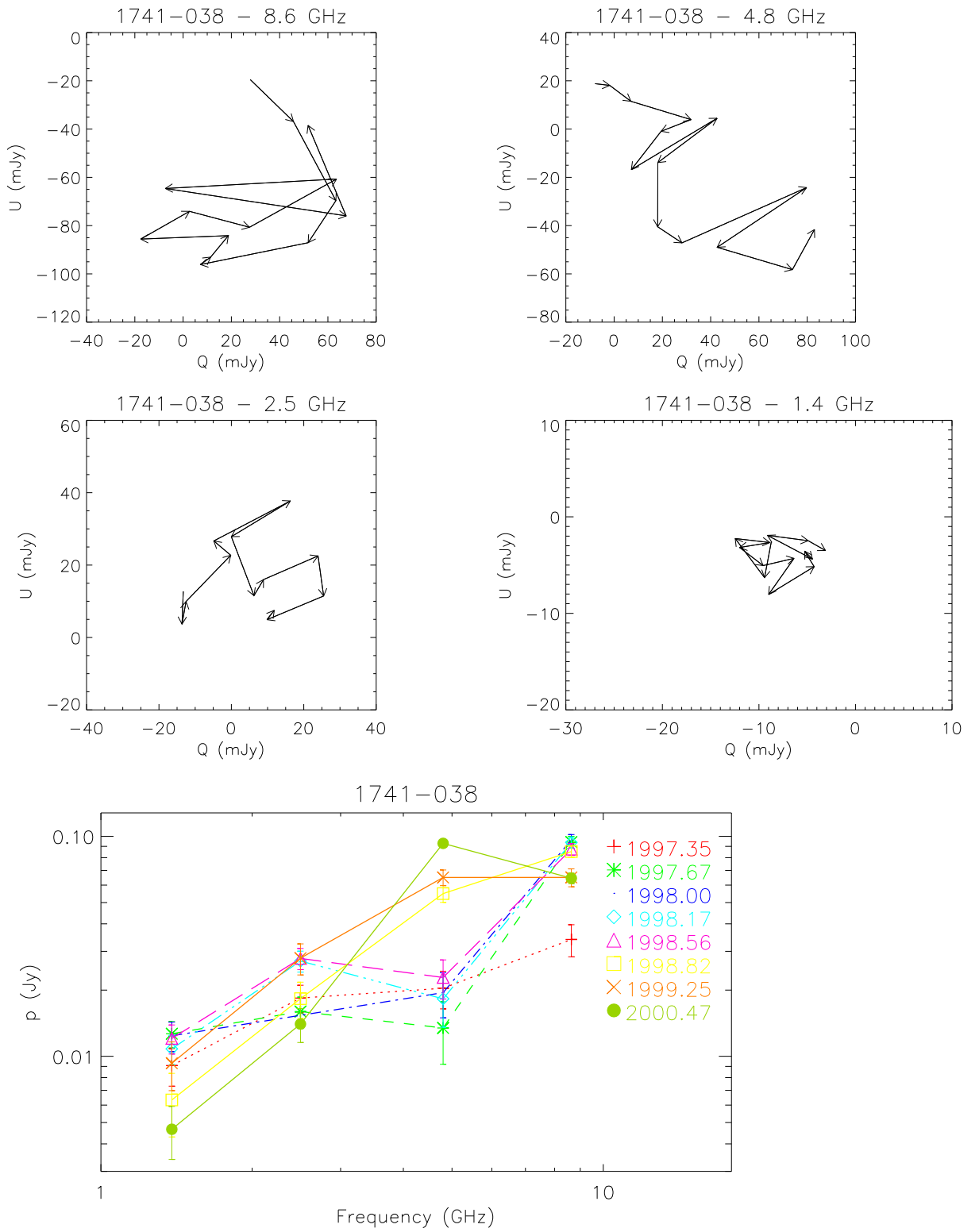
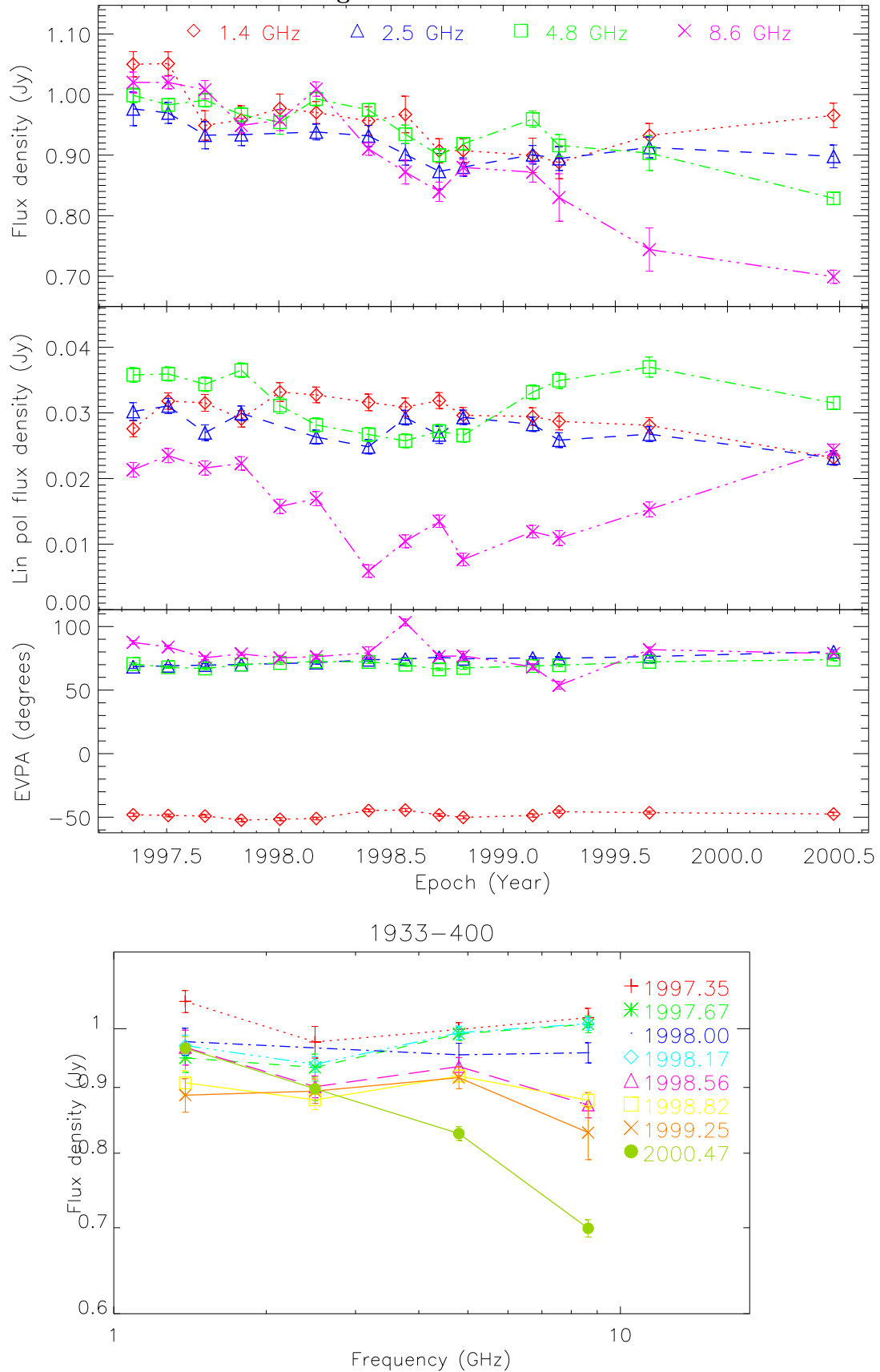


Figure A.15: PKS 1933–400



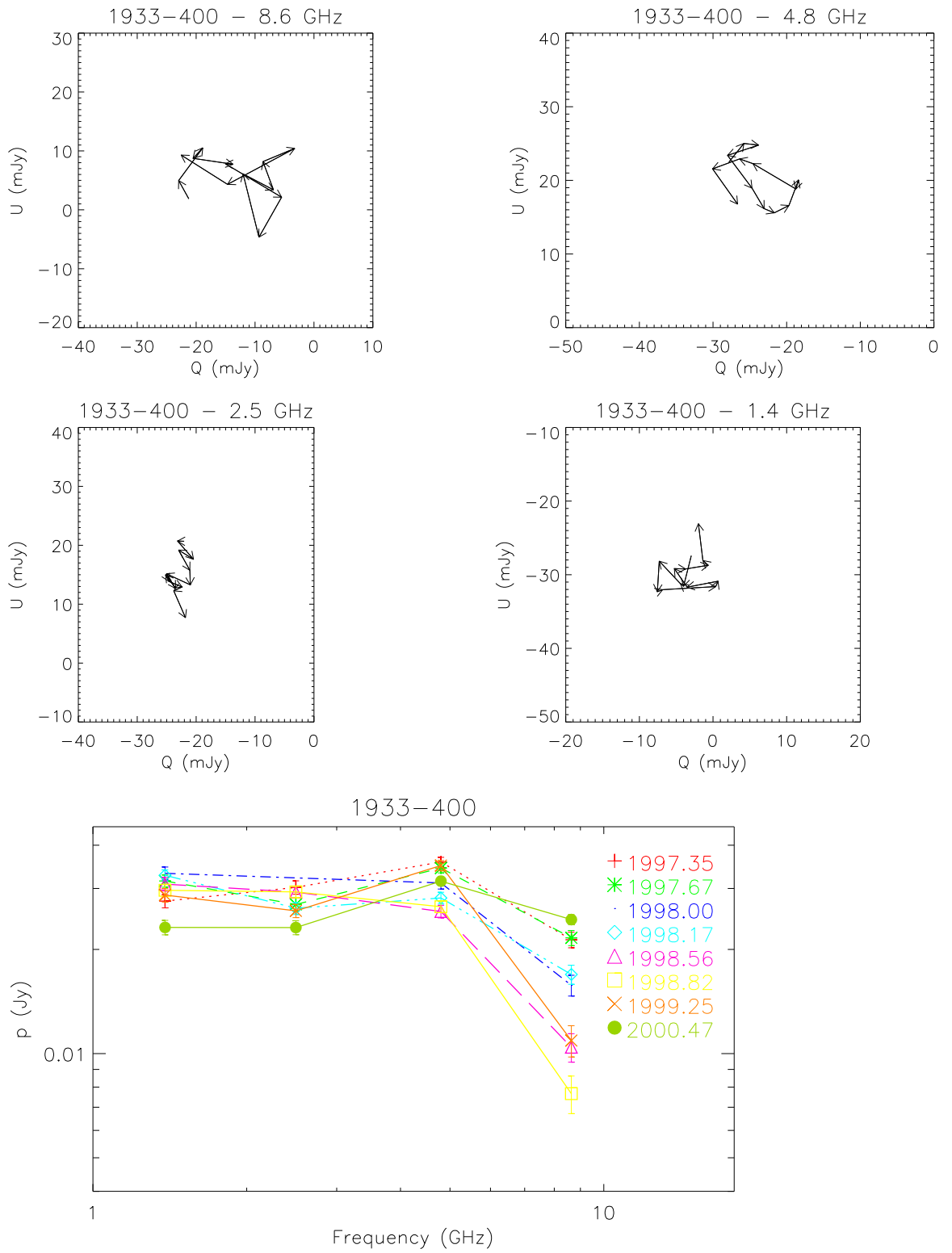
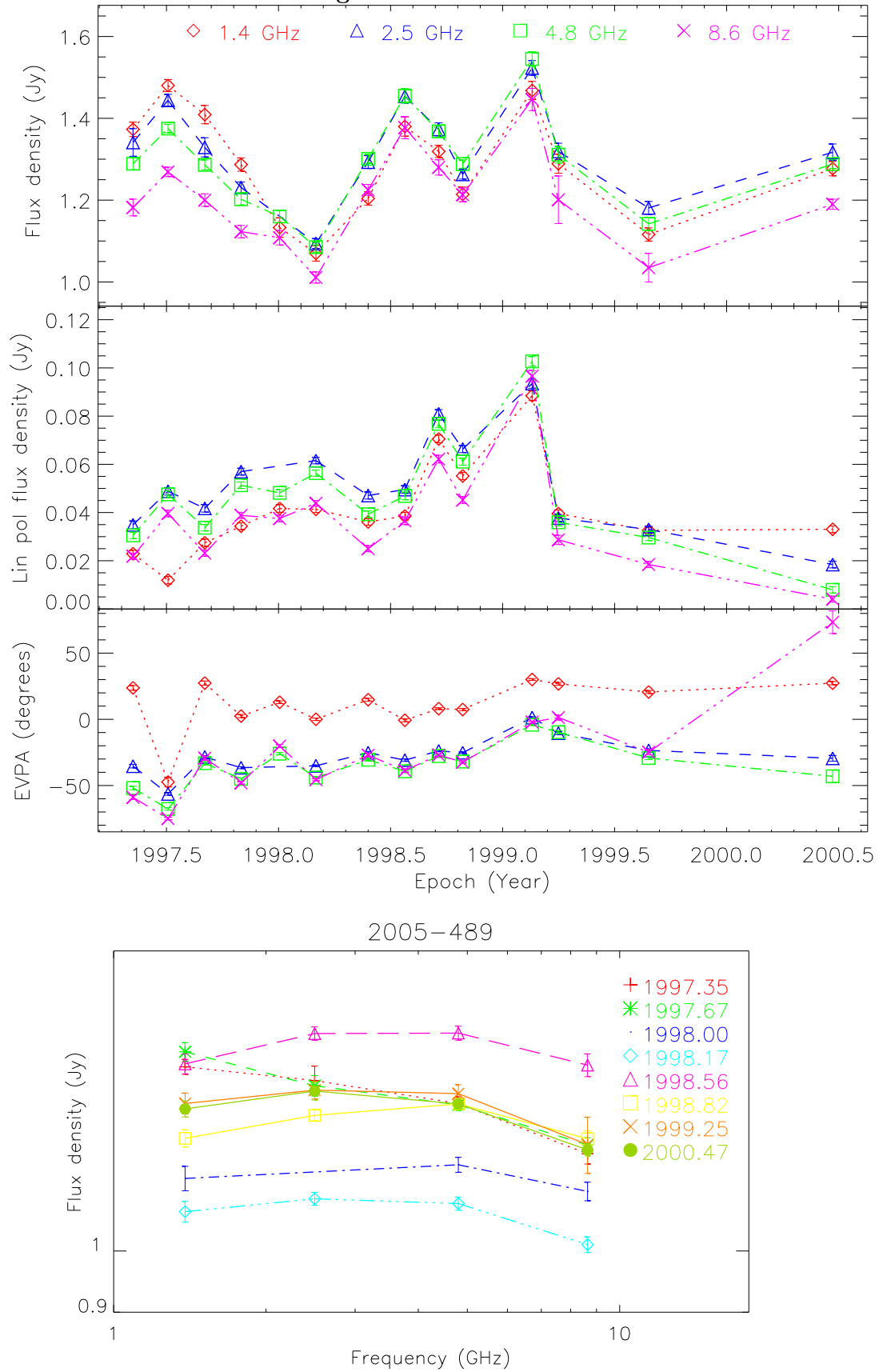


Figure A.16: PKS 2005–489



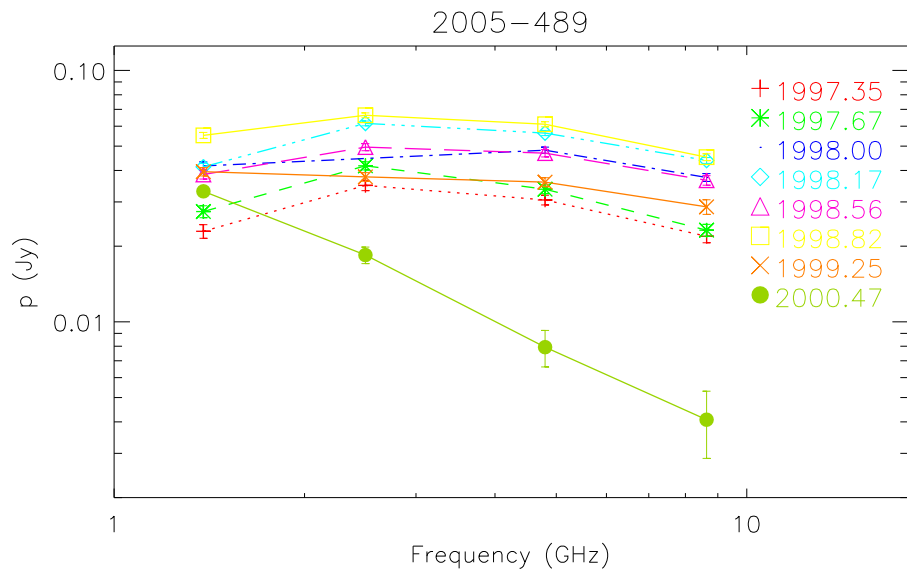
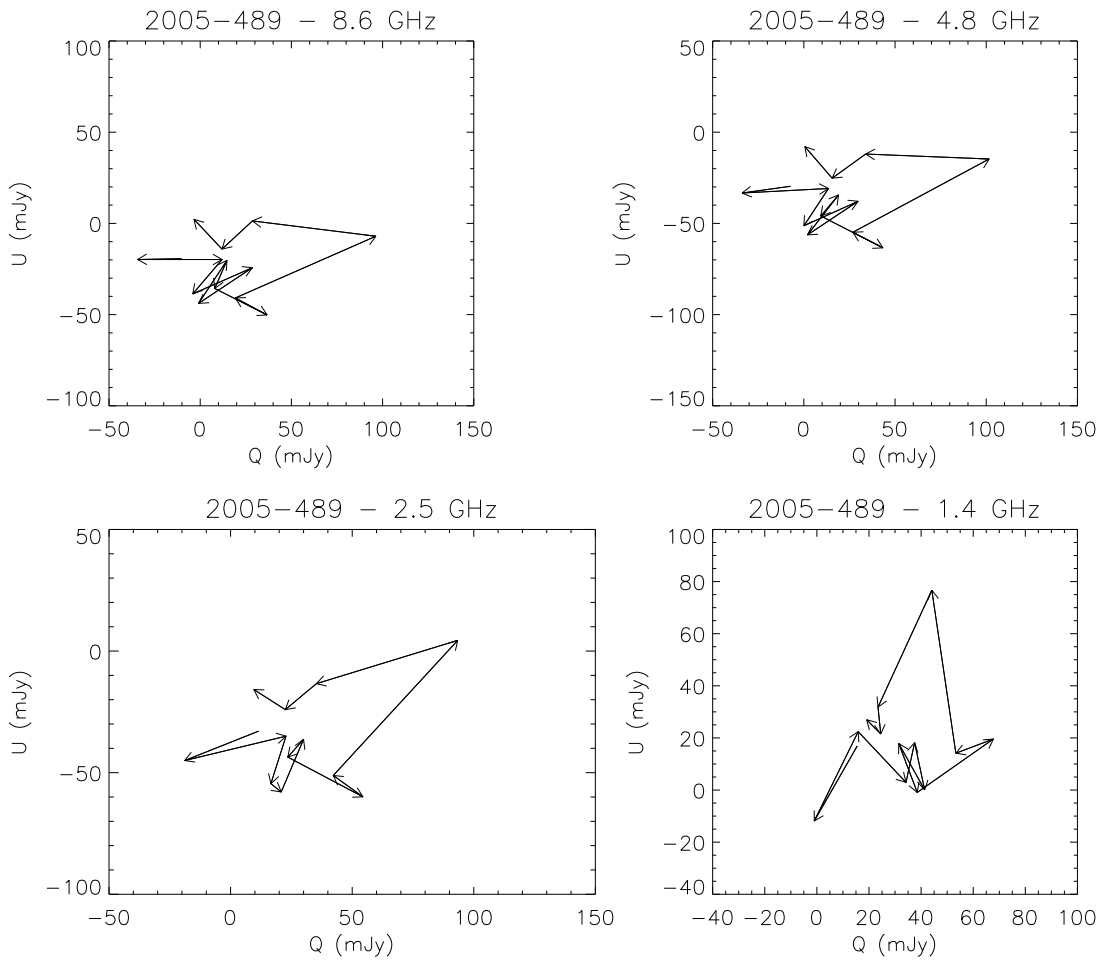
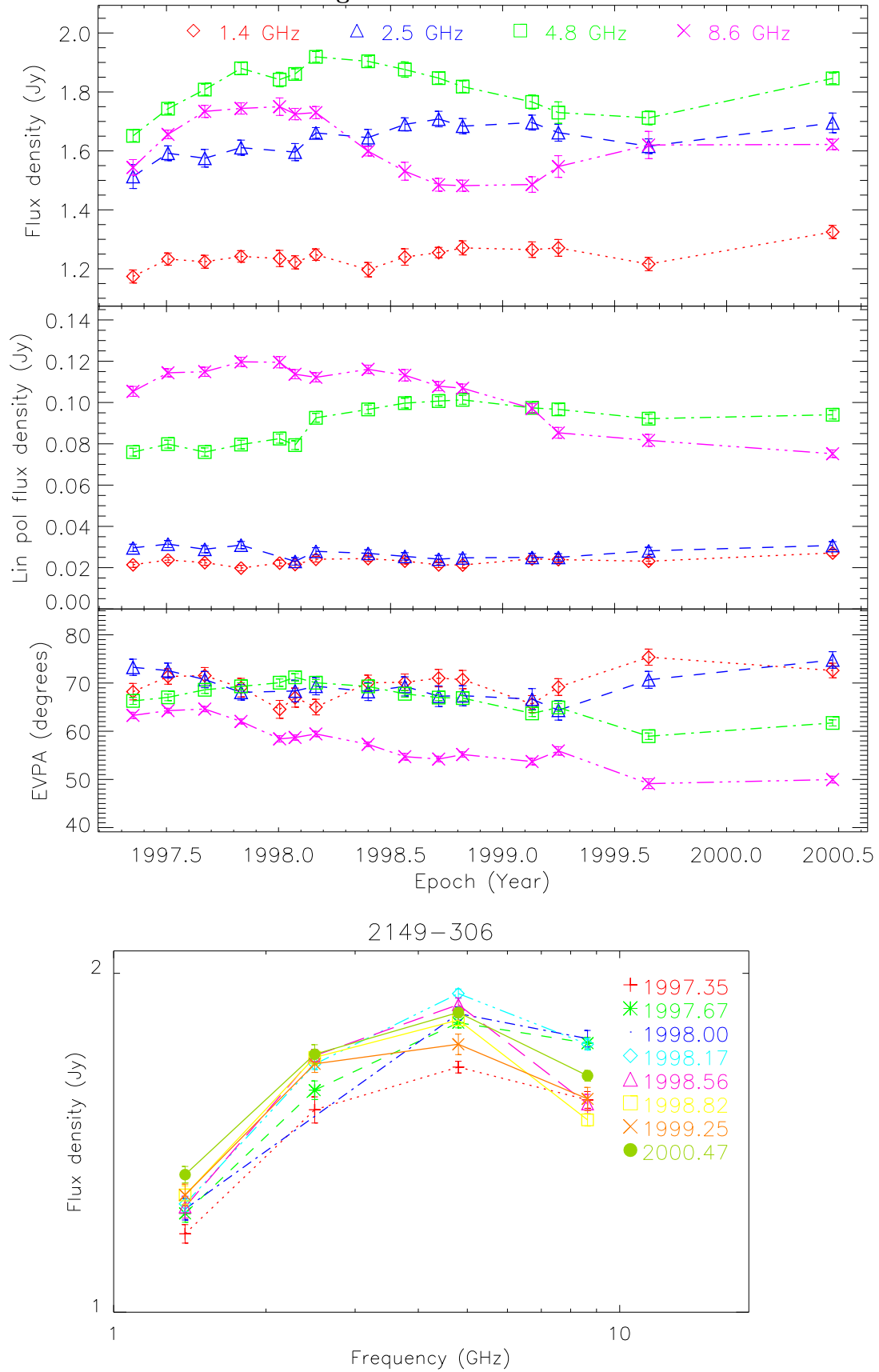


Figure A.17: PKS 2149–306



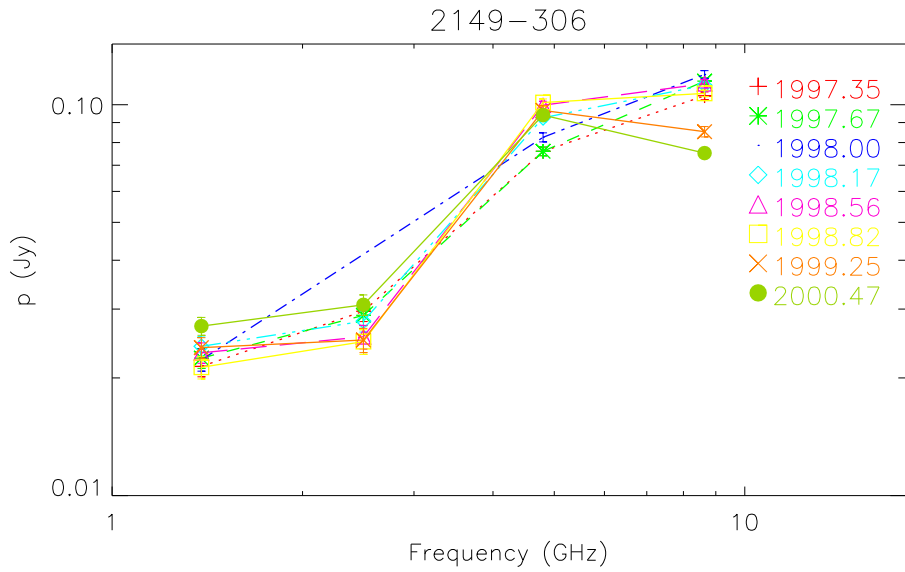
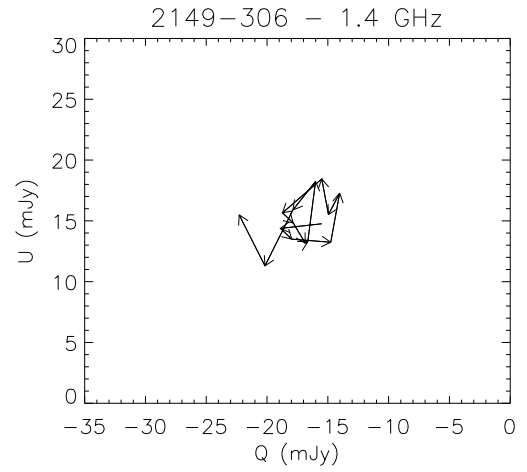
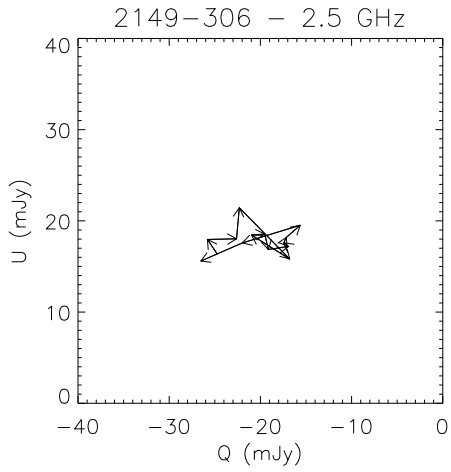
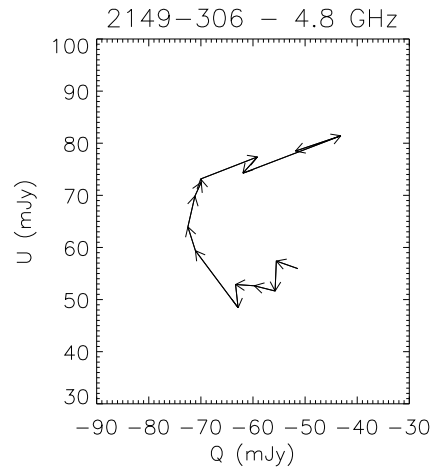
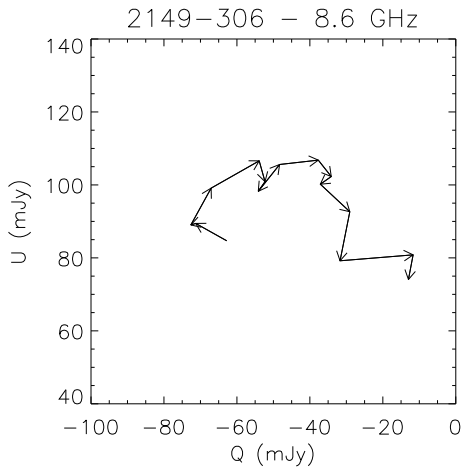
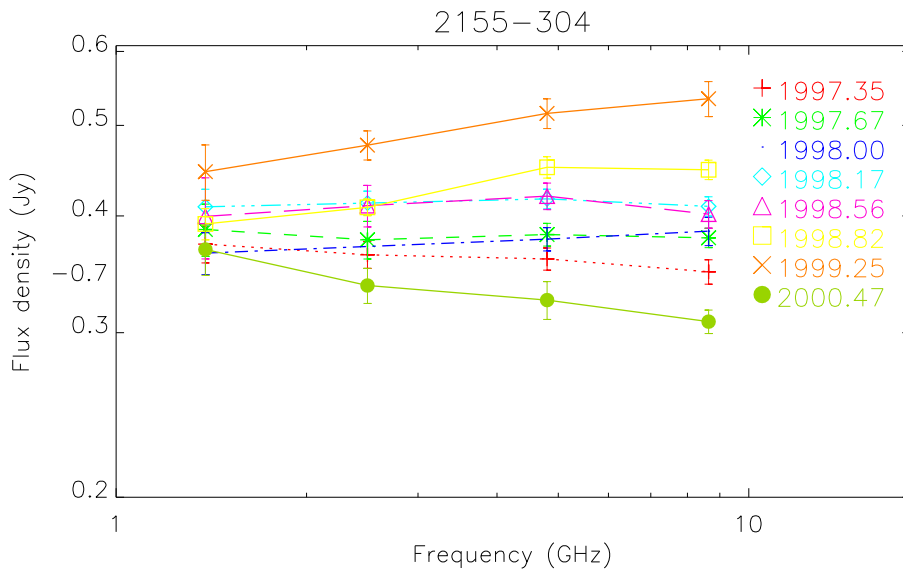
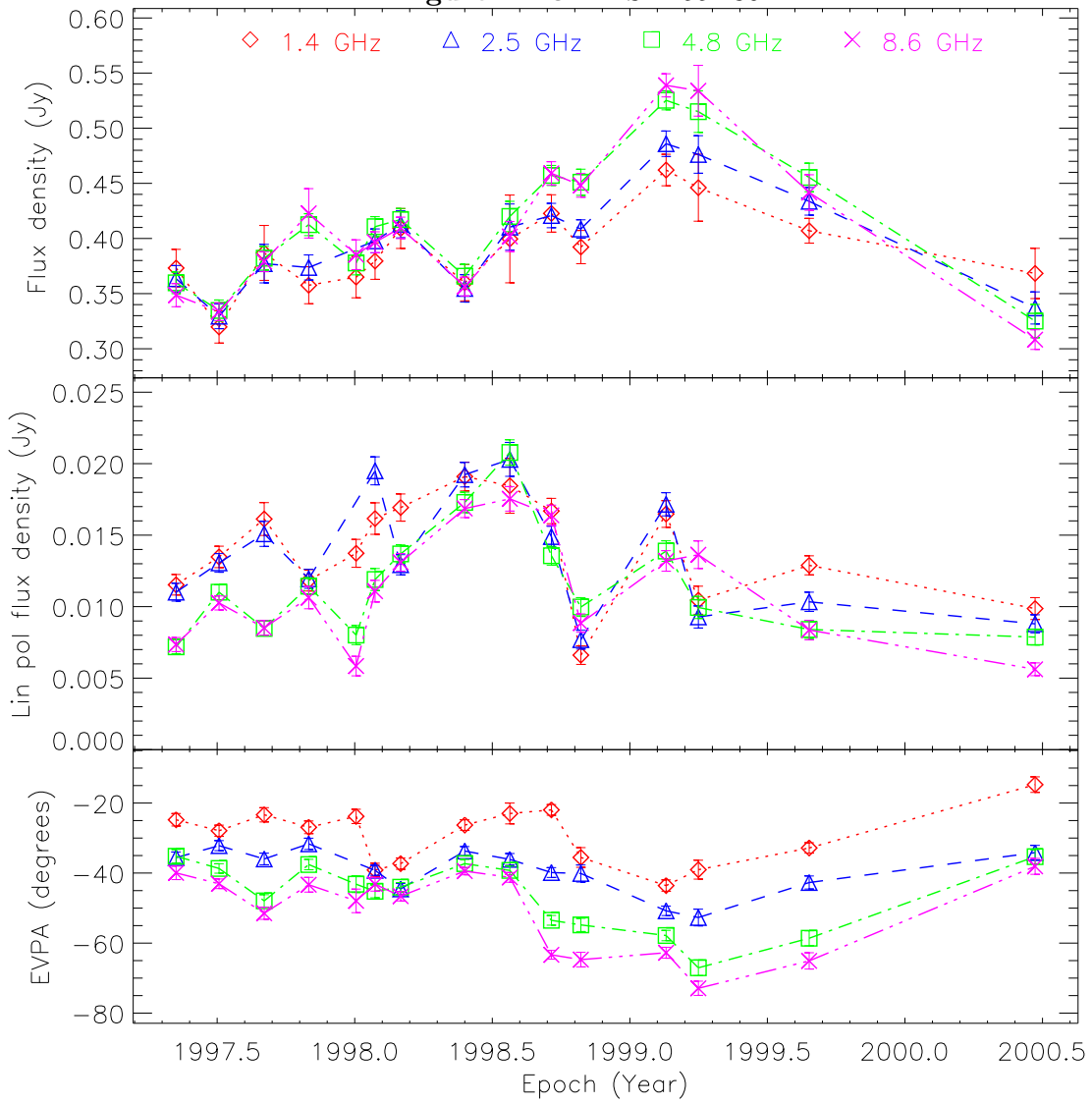


Figure A.18: PKS 2155–304



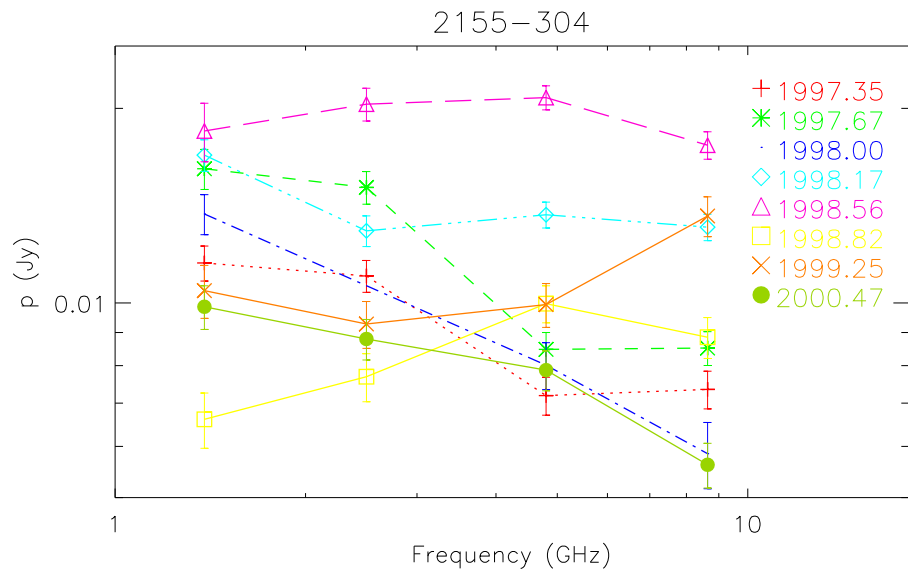
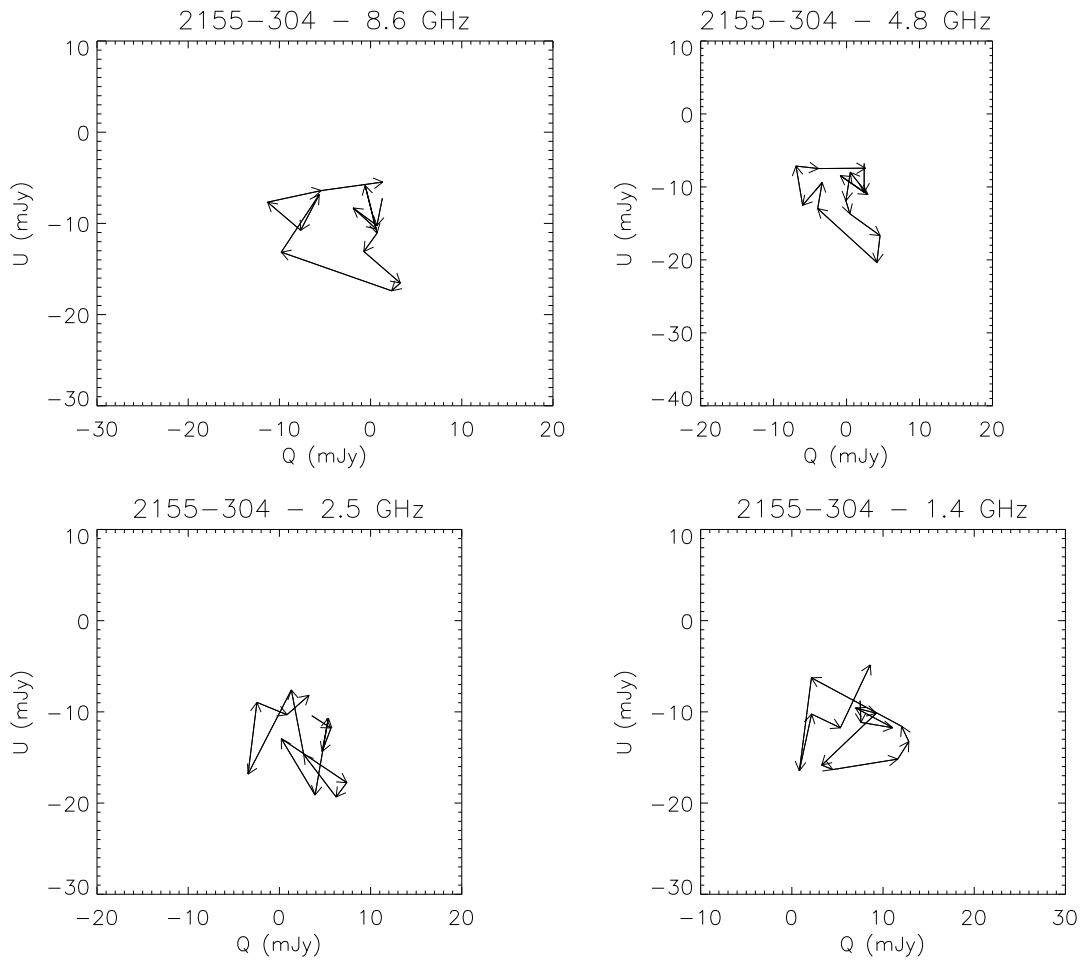
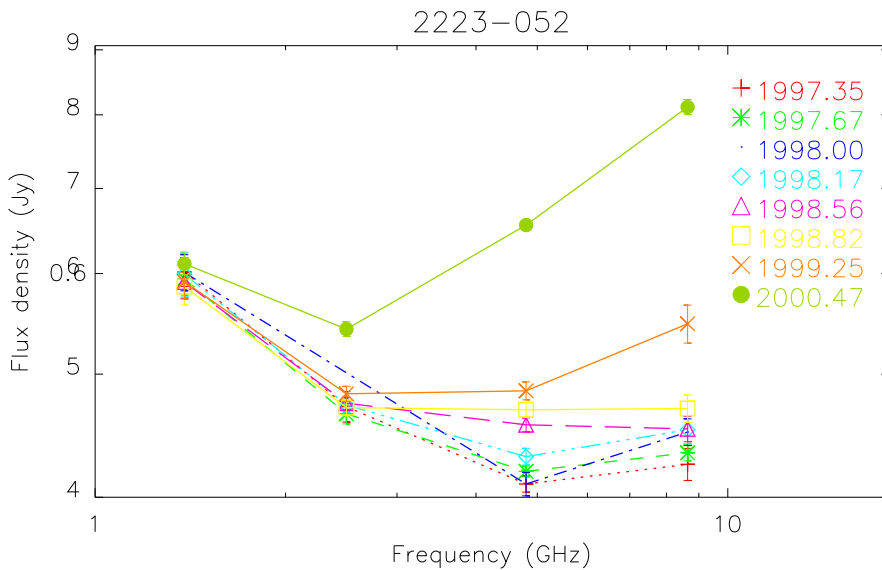
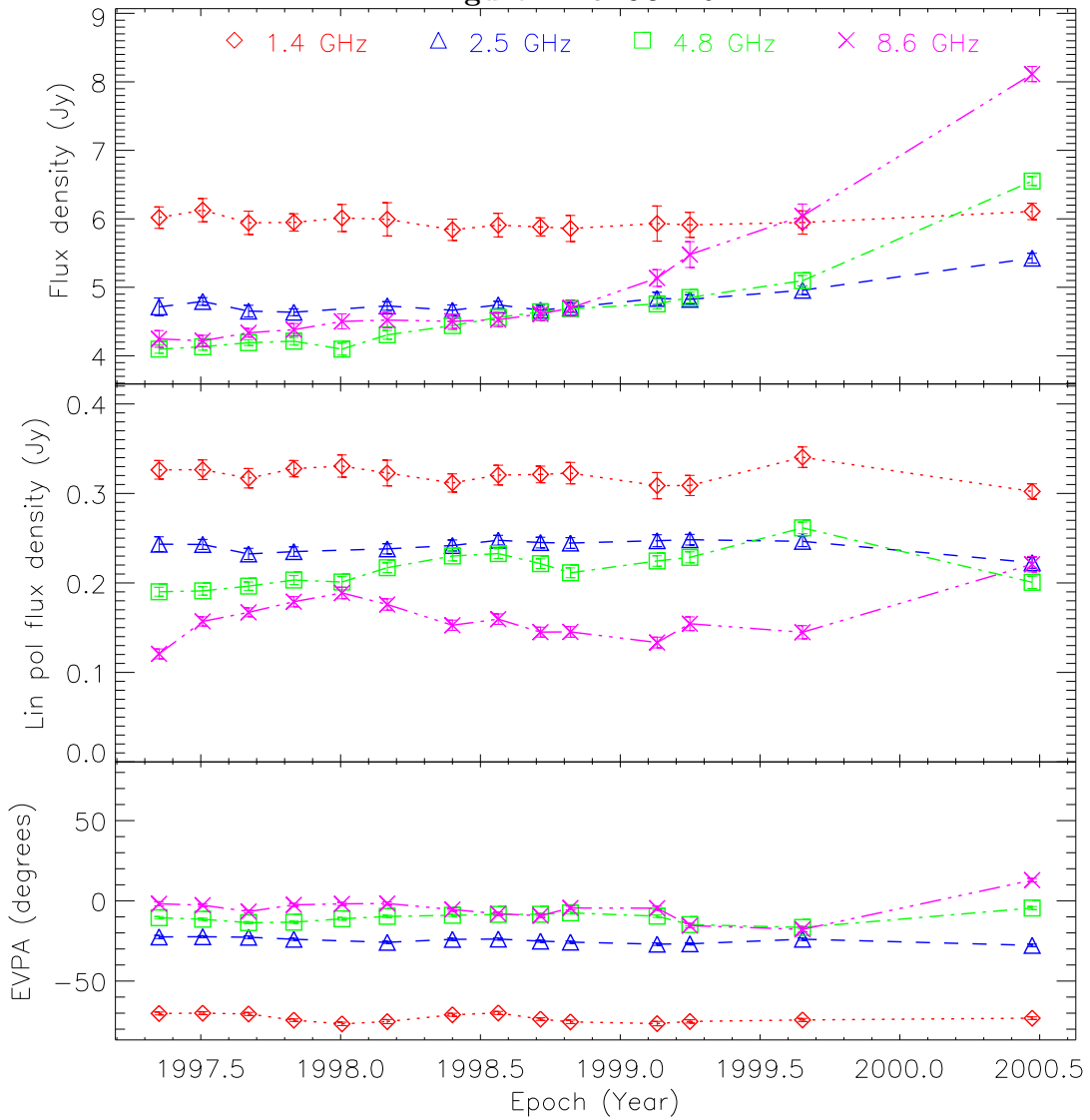


Figure A.19: 3C 446



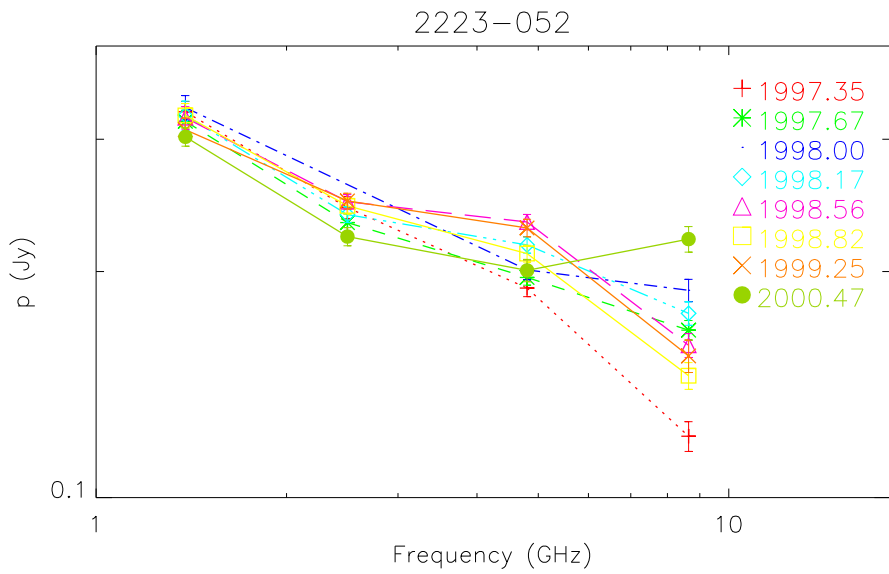
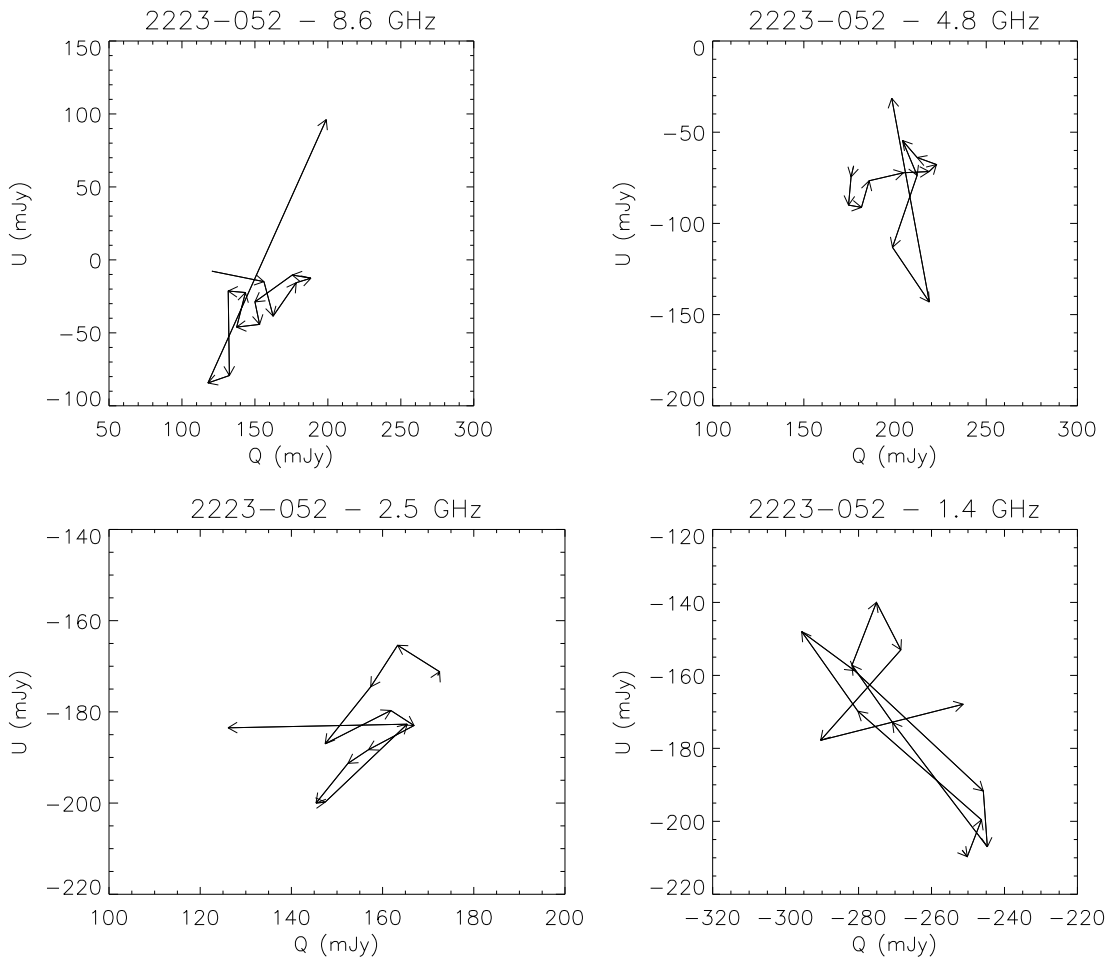
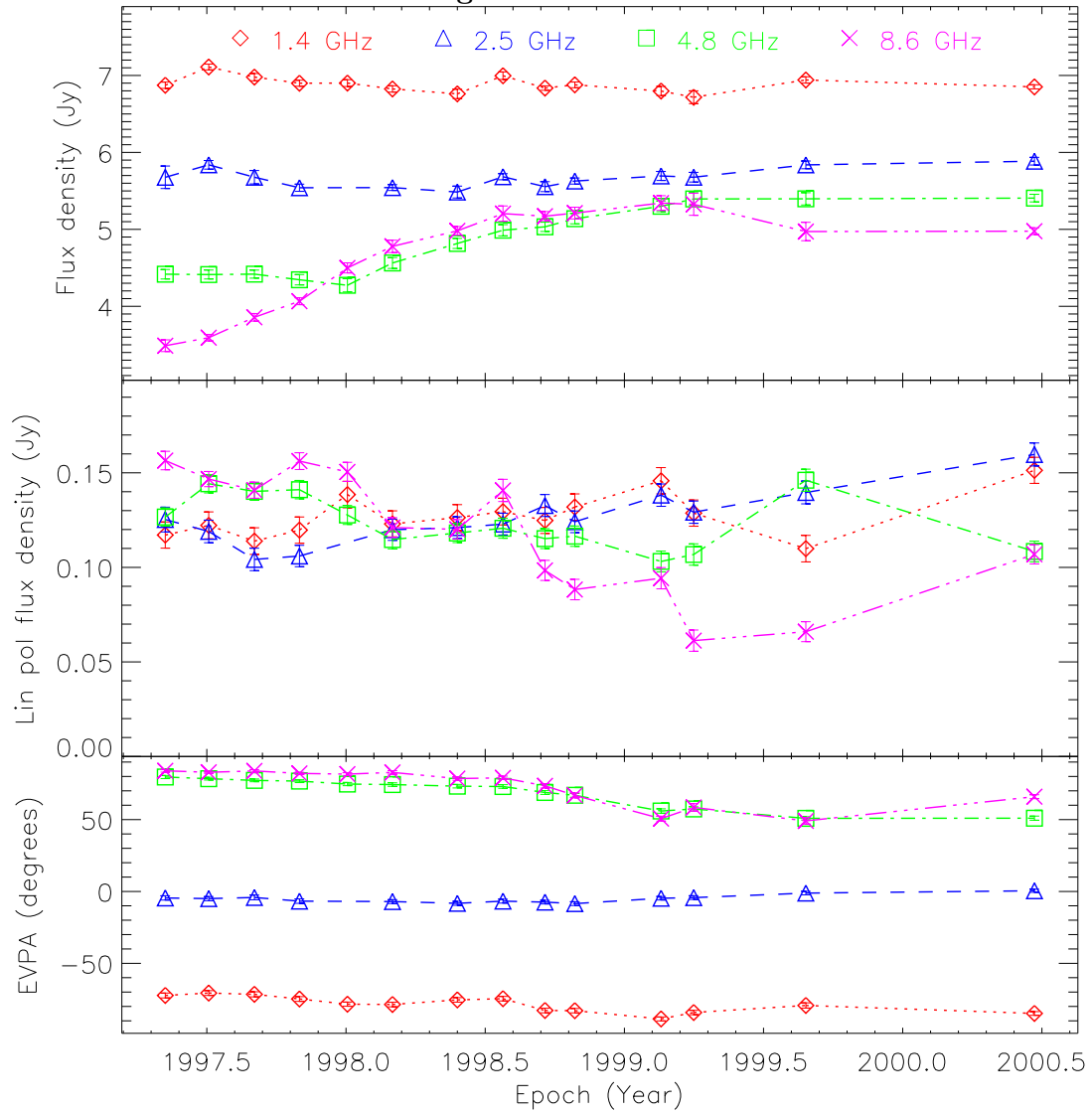
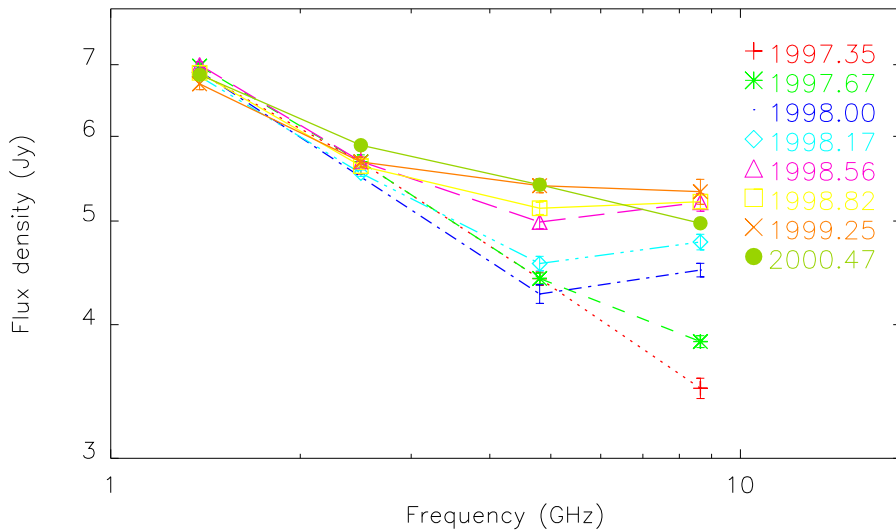


Figure A.20: CTA 102



2230+114



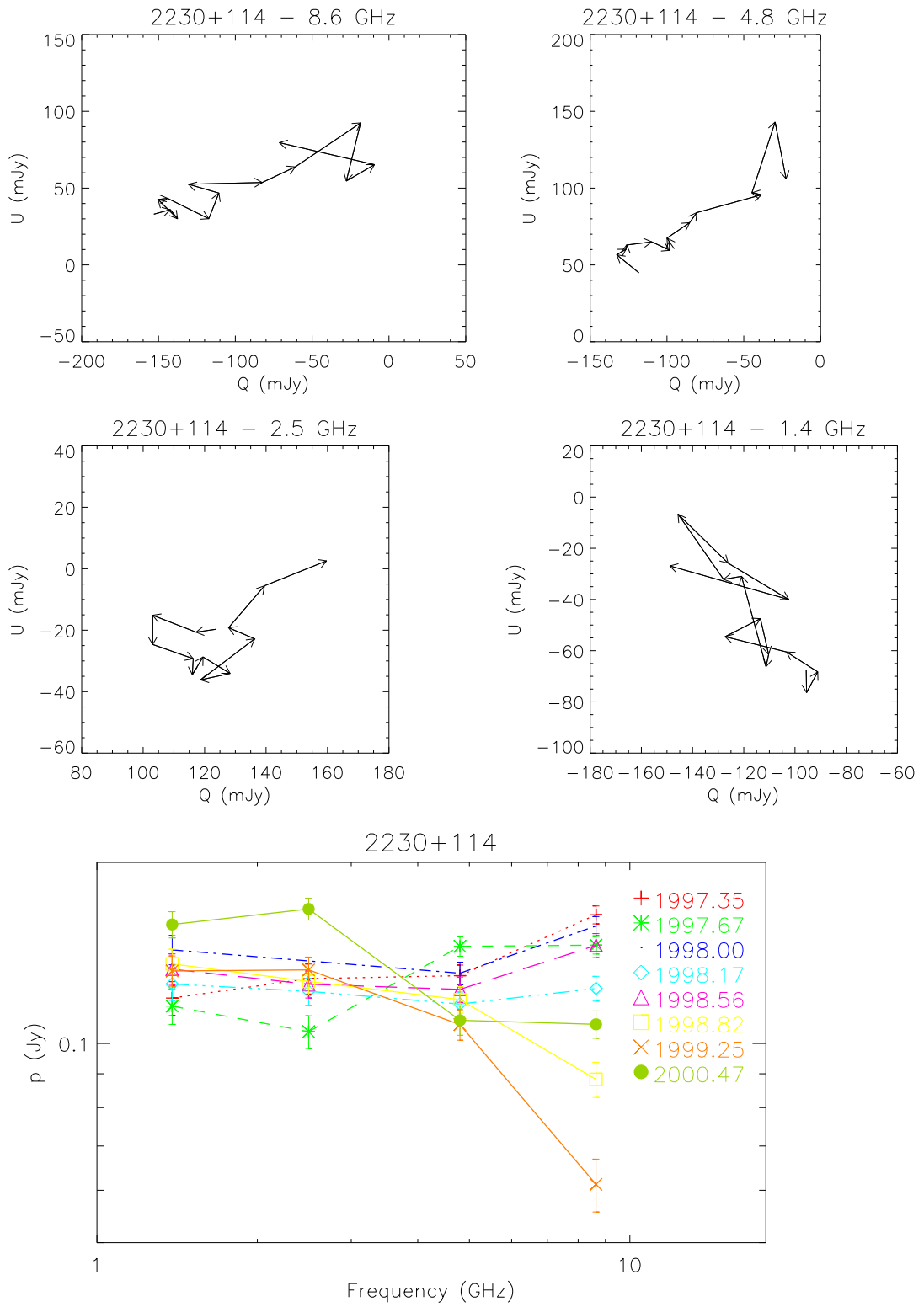
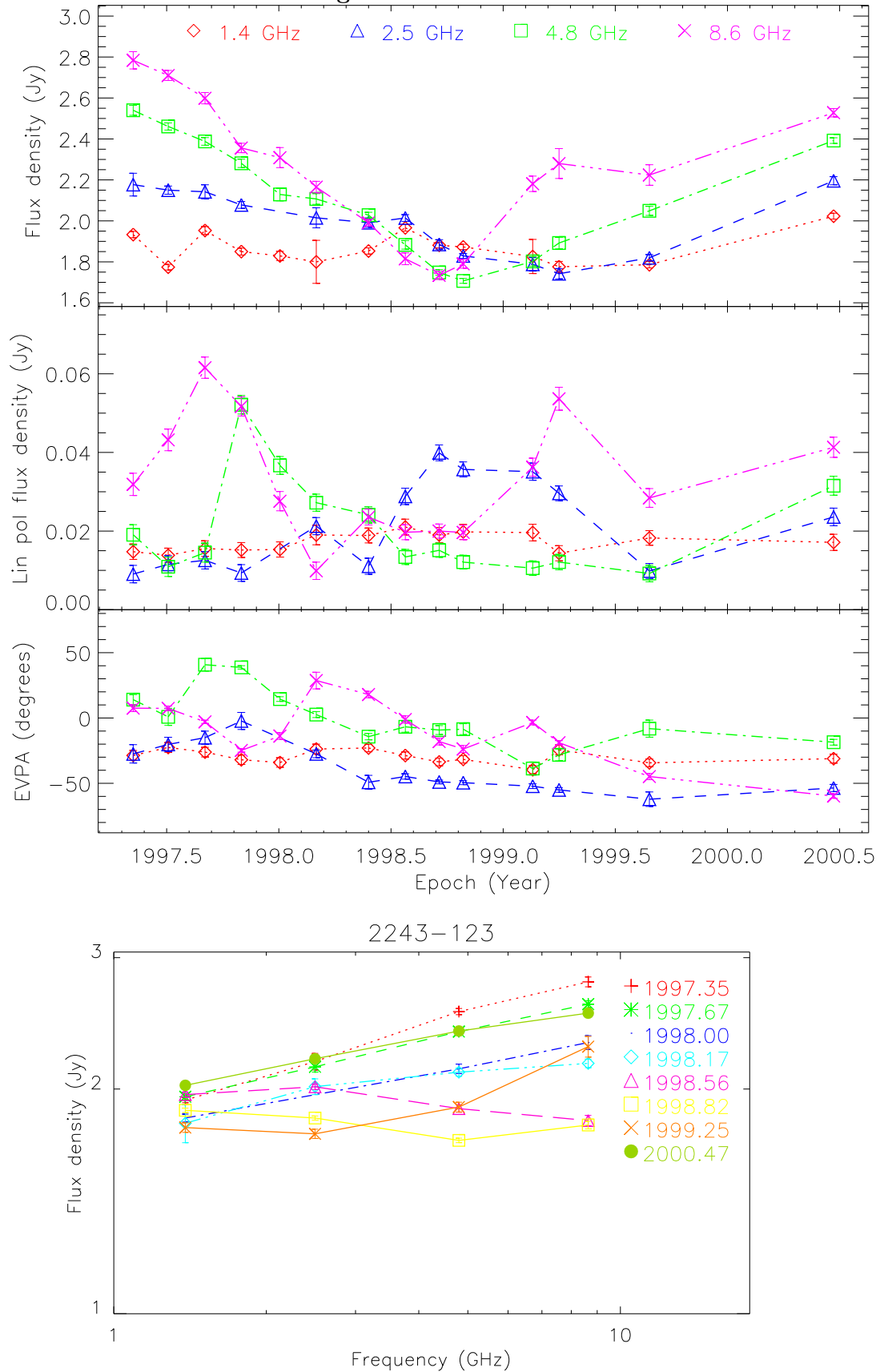


Figure A.21: PKS 2243–123



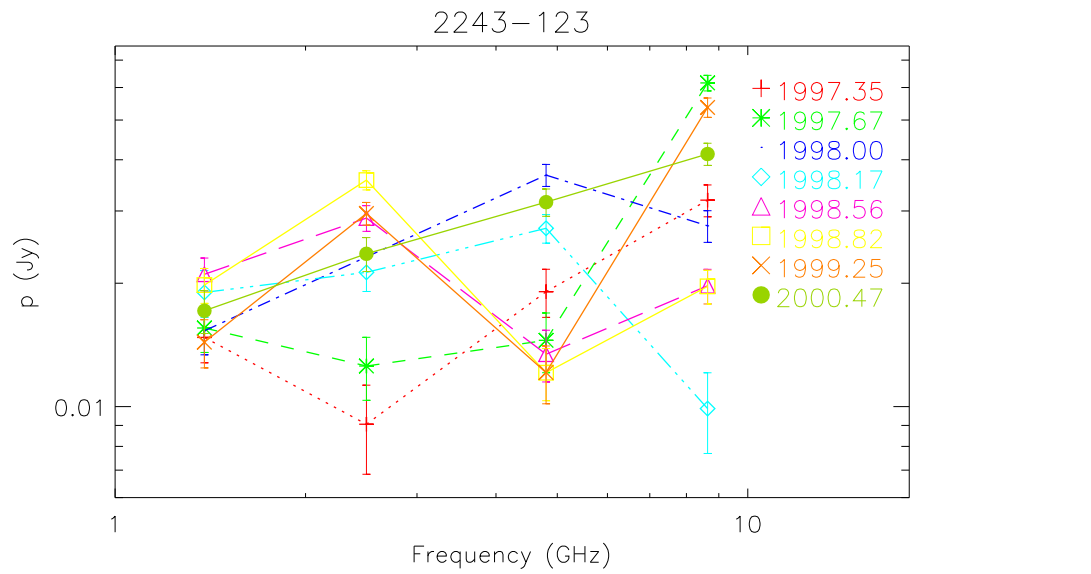
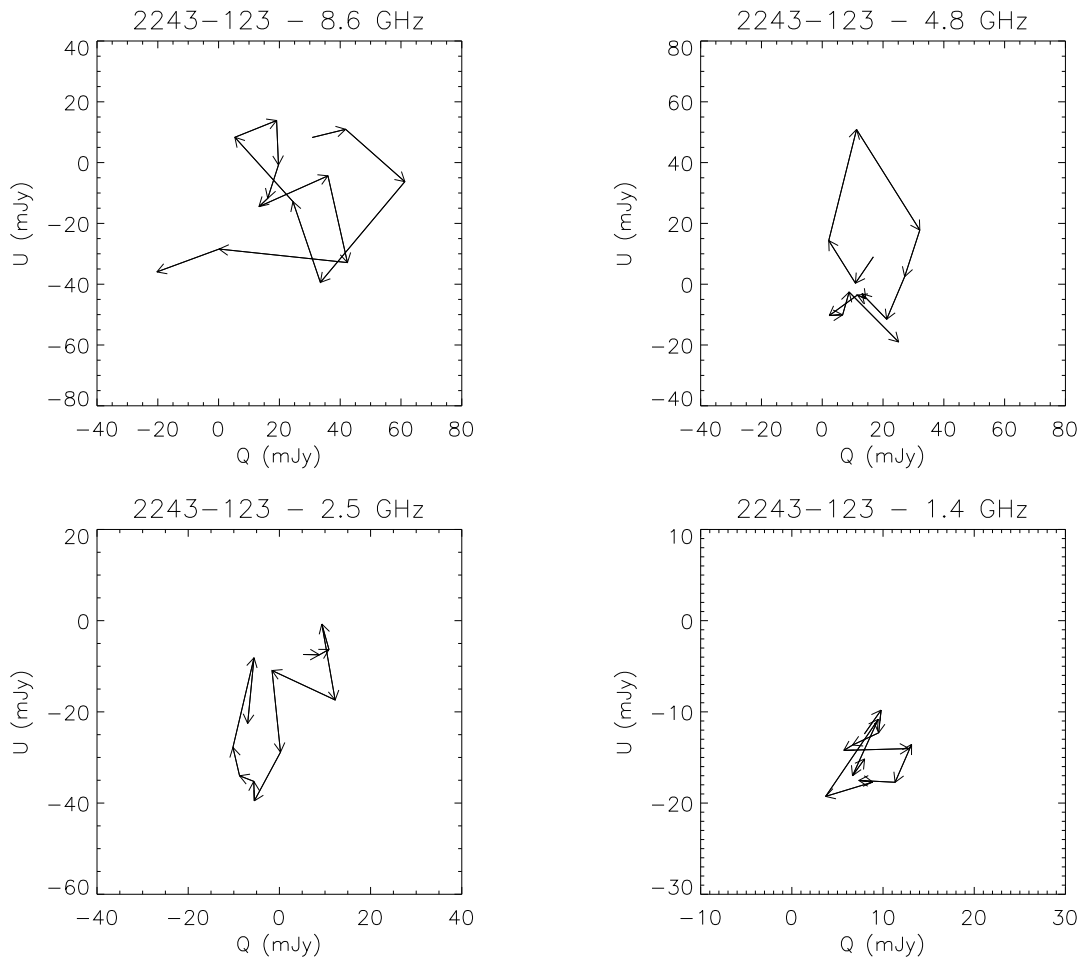
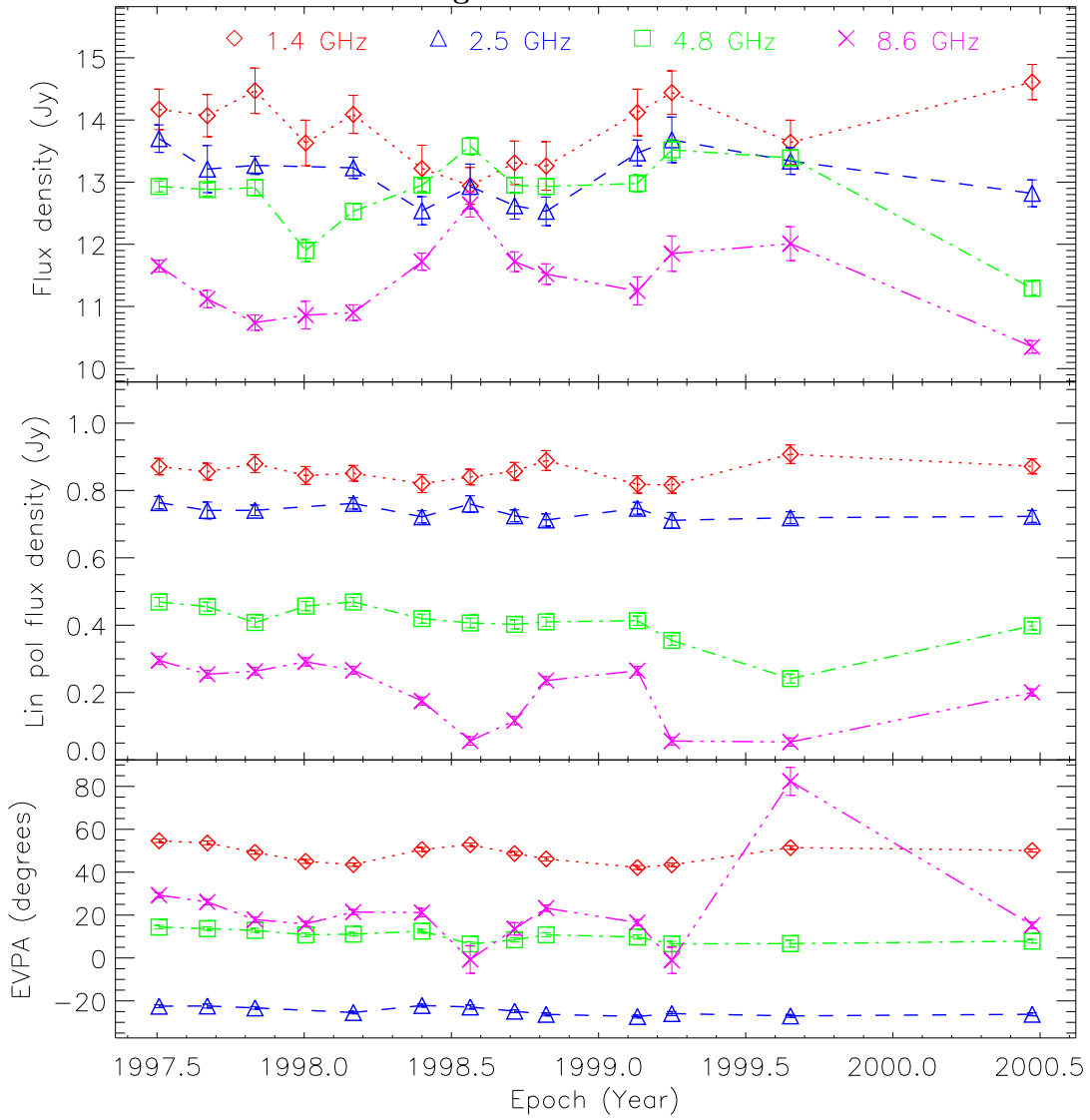
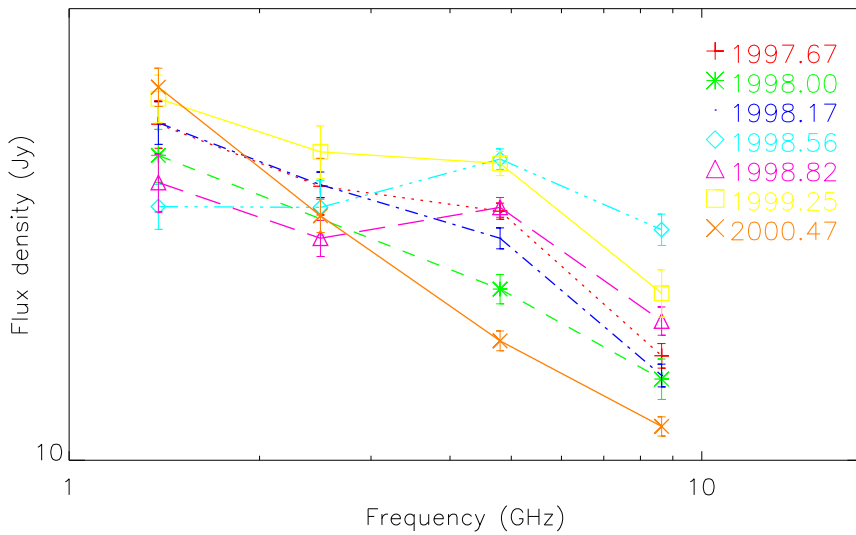
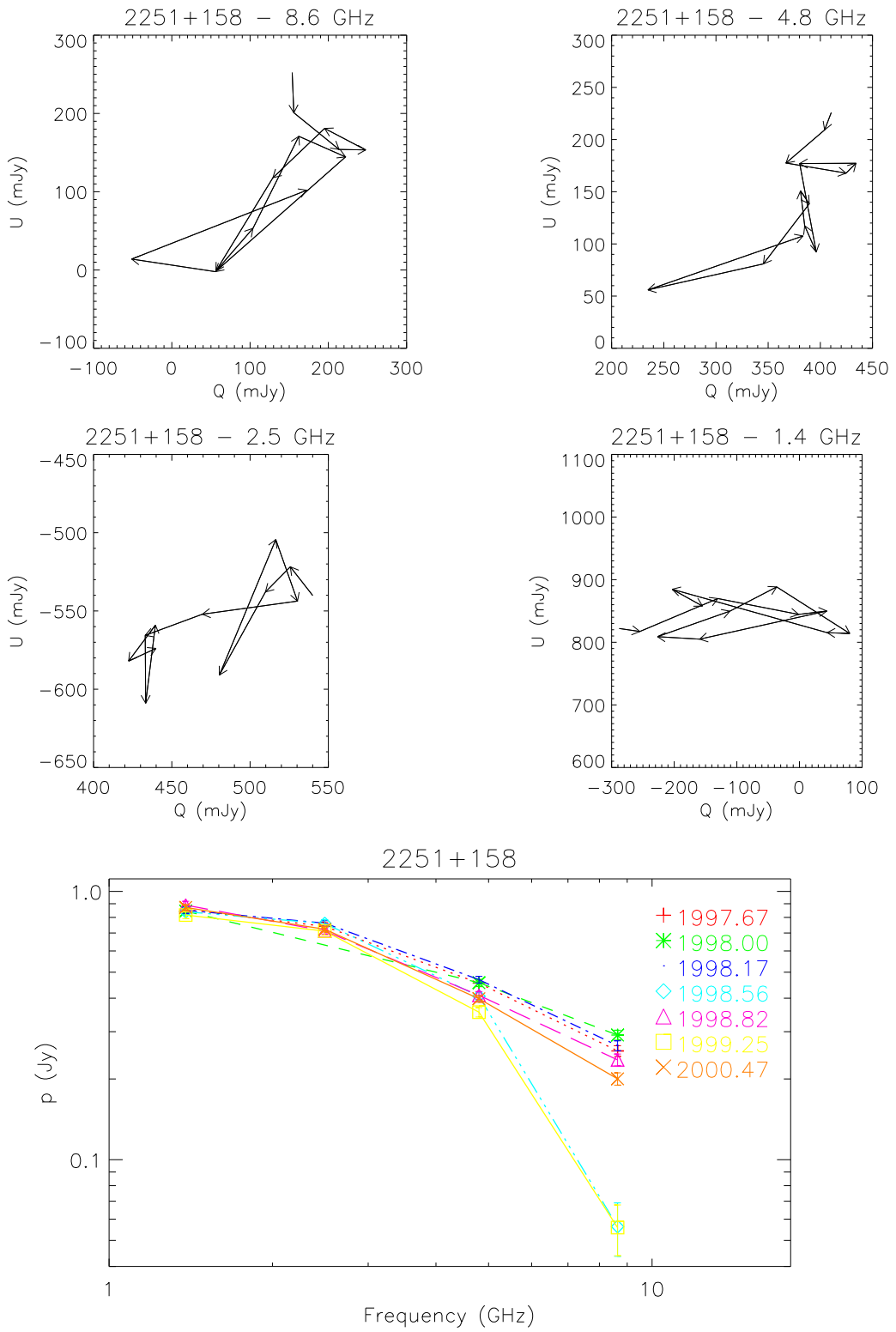


Figure A.22: 3C 454.3



2251+158





Appendix B

ATCA data on other blazars

This section presents average flux densities measured for blazars observed in ATCA project C639 but which were not part of the “core sample” presented in Chapters 3 and 4.

Table B.1: Additional sources observed with the ATCA for project C639. “ID” is classification from available literature. HBL = high-frequency peaked BL Lac object; LBL = low-frequency peaked BL Lac object; HPQ = high optically polarized quasar; LPQ = low optically polarized quasar; Q=quasar (optical polarization not available); RG = radio galaxy; Sy1 = Seyfert 1

Catalog name	(B1950)	RA (J2000)	Dec (J2000)	z	ID
1ES 0120+340		01:23:08.55	+34:20:47.5	0.272	HBL
1ES 0145+138		01:48:32.21	+14:02:30.1	0.125	HBL
MS 0158+002		01:58:32.14	+00:19:33.8	0.299	HBL
3C 66A	0219+428	02:22:39.62	+43:02:08.6	0.444	LBL
RBS 0319	0224+014	02:27:16.58	+02:02:00.1	...	HBL
CTD 20	0234+285	02:37:52.41	+28:48:09.0	1.213	HPQ
MS 0317+183		03:19:51.22	+18:45:36.9	0.190	HBL
1ES 0323+022		03:26:13.96	+02:25:14.7	0.147	HBL
1ES 0347-121		03:49:23.01	-11:59:27.9	0.188	HBL
1ES 0414+009		04:16:52.38	+01:05:24.0	0.287	HBL
PKS 0446+112		04:49:07.67	+11:21:28.7	1.207	RG
1ES 0507-040		05:09:38.14	-04:00:45.5	0.304	HBL
PKS 0521-365		05:22:57.98	-36:27:30.8	0.055	BL
PKS 0537-441		05:38:50.36	-44:05:08.9	0.894	LBL
PMN J0546-6415	0546-642	05:46:41.80	-64:15:21.0	0.323	BL
PKS 0548-322		05:50:40.59	-32:16:47.06	0.069	HBL
PKS 0637-752		06:35:46.51	-75:16:16.8	0.653	Q
PKS 0735+178		07:38:07.39	+17:42:19.0	0.424	LBL
OJ 287	0851+202	08:54:48.87	+20:06:30.6	0.306	LBL
B2 0912+29	0912+297	09:15:52.40	+29:33:24.0	...	LBL
1ES 1101-232		11:03:37.57	-23:29:30.2	0.186	HBL
Mkn 421	1101+384	11:04:27.28	+38:12:32.3	0.031	HBL
1ES 1118+424		11:20:48.08	+42:12:12.2	0.124	HBL
ON 325	1215+303	12:17:52.08	+30:07:00.9	0.130	BL
W COMAE	1219+285	12:21:31.69	+28:13:58.5	0.102	LBL
3C 273	1226+023	12:29:06.70	+02:03:08.6	0.158	LPQ
1ES 1255+244		12:57:31.70	+24:12:44.2	0.141	HBL
1ES 1312-422		13:15:03.68	-42:36:50.2	0.105	HBL
1ES 1320+084		13:22:54.90	+08:10:10.0	0.050	Sy1
PG 1424+240		14:29:16.50	+23:34:40.0	...	LBL
PKS 1510-089		15:12:50.53	-09:05:59.8	0.360	HPQ
1ES 1553+113		15:55:43.11	+11:11:24.1	0.360	HBL
B2 1633+38	1633+380	16:35:15.51	+38:08:04.7	1.814	LPQ
3C 345	1641+399	16:42:58.82	+39:48:37.2	0.594	HPQ
Mkn 501	1652+398	16:53:52.23	+39:45:36.8	0.055	HBL
1ES 1741+196		17:43:57.83	+19:35:09.0	0.084	HBL
PKS 1749+096		17:51:32.82	+09:39:00.7	0.322	BL
PKS 2128-123		21:31:35.26	-12:07:04.8	0.501	LPQ
BL LAC	2200+420	22:02:43.30	+42:16:39.7	0.069	LBL
PKS 2255-282		22:58:05.96	-27:58:21.3	0.926	LPQ
RBS 2070	2356-309	23:59:07.83	-30:37:39.0	0.165	HBL

Table B.2: Mean radio properties for additional blazars observed in ATCA project C639, at 1.4, 2.5, 4.8 and 8.6 GHz. Flux density is the flux density of the unresolved “core” component only. α is the mean spectral index, where $S_\nu \propto \nu^\alpha$. $S_{\text{ext}}/S_{\text{tot}}$ is the percentage of extended emission or confusion estimated from the closure phases, where signal-to-noise is sufficient (i.e. for sources stronger than ~ 100 mJy). For very extended sources there are significant uncertainties in $S_{\text{ext}}/S_{\text{tot}}$, but the numbers provide a good indication of which sources are compact and which are significantly extended or confused. “ext” in these columns indicates sources dominated by an extended component.

IAU name (B1950)	Flux density (Jy)				α		$S_{\text{ext}}/S_{\text{tot}}$ (%)			
	1.4	2.5	4.8	8.6	$\alpha_{1.4}^{4.8}$	$\alpha_{4.8}^{8.6}$	1.4	2.5	4.8	8.6
0120+340	0.032	0.028	0.026	0.023	-0.16	-0.21
0145+138	0.023	0.006	0.005	0.004	-1.23	-0.38
0158+002	<0.003	<0.001	<0.001	<0.001
0219+428	1.42	1.28	1.15	1.03	-0.16	-0.17	23	14	7.5	5.1
0224+014	0.030	0.025	0.016	0.012	-0.51	-0.49
0234+285	1.99	1.85	1.92	2.03	-0.03	0.08	2.8	1.5	0.8	1.0
0317+183	0.14	0.080	0.022	0.014	-1.49	-0.77	36	46
0323+022	0.060	0.052	0.040	0.042	-0.33	0.08
0347-121	0.025	0.011	0.009	0.008	-0.82	-0.20
0414+009	0.071	0.067	0.057	0.053	-0.18	-0.12
0446+112	0.79	0.78	0.95	1.22	0.15	0.44	26	19	3.9	1.1
0507-040	0.038	0.035	0.023	0.020	-0.40	-0.24
0521-365	6.80	3.75	2.93	2.80	-0.68	-0.08	ext	ext	80	40
0537-441	2.59	3.07	4.10	4.94	0.35	0.33	4.1	2.9	1.3	0.9
0546-642	0.15	0.23	0.17	0.12	0.13	-0.71	35	9.3	6.1	15
0548-322	0.16	0.11	0.074	0.057	-0.62	-0.44	63	43	39	60
0637-752	4.26	5.35	6.25	5.87	0.31	-0.10	14	7.1	3.6	2.4
0735+178	1.21	1.19	1.13	1.00	-0.06	-0.21	6.5	2.2	0.9	1.3
0851+202	1.22	1.56	1.92	2.13	0.37	0.18	6.3	4.0	1.1	0.8
0912+297	0.30	0.23	0.19	0.16	-0.36	-0.33	17	13	9.6	8.2
1101-232	0.081	0.063	0.052	0.042	-0.36	-0.36
1101+384	0.58	0.59	0.62	0.59	0.05	-0.08	7.9	3.1	1.5	1.3
1118+424	0.027	0.023	0.022	0.021	-0.16	-0.08
1215+303	0.36	0.37	0.39	0.39	0.07	-0.01	8.0	4.0	2.3	2.6
1219+285	0.82	0.78	0.76	0.73	-0.06	-0.07	10	5.5	1.5	1.3
1226+023	37.9	35.4	31.1	31.1	-0.16	0.00	47	30	15	7.2
1255+244	0.015	0.009	0.008	0.007	-0.51	-0.23
1312-422	0.017	0.014	0.013	0.012	-0.22	-0.13
1320+084	0.008	0.013	0.011	0.008	0.26	-0.54
1424+240	0.35	0.27	0.26	0.24	-0.24	-0.16	52	7.1	4.6	12
1510-089	2.17	1.87	1.78	1.73	-0.16	-0.04	3.7	5.0	3.5	2.7
1553+113	0.25	0.25	0.26	0.26	0.00	-0.12	49	43	26	7.6
1633+382	2.91	2.67	2.44	2.21	-0.14	-0.17	1.5	0.8	0.6	0.7
1641+399	6.93	7.63	8.18	7.74	0.13	-0.09	1.0	2.4	3.2	2.3

IAU name (B1950)	Flux density (Jy)				α		$S_{\text{ext}}/S_{\text{tot}}$ (%)			
	1.4	2.5	4.8	8.6	$\alpha_{1.4}^{4.8}$	$\alpha_{4.8}^{8.6}$	1.4	2.5	4.8	8.6
1652+398	1.68	1.59	1.58	1.44	-0.05	-0.16	4.3	3.9	3.1	1.0
1741+196	0.23	0.20	0.19	0.18	-0.12	-0.22	25	15	9.6	20
1749+096	1.16	1.90	3.18	3.81	0.81	0.31	12	2.3	0.5	0.8
2128-123	1.71	2.04	2.72	2.86	0.37	0.07	3.7	1.8	0.8	0.8
2200+420	4.04	3.80	3.96	4.03	-0.02	0.03	1.3	0.8	0.7	1.0
2255-282	1.16	1.81	3.66	5.97	0.92	0.84	5.7	2.3	0.9	0.7
2356-309	0.040	0.039	0.037	0.033	-0.06	-0.19

Table B.3: Mean linear polarization for blazars observed in ATCA project C639, which are core-dominated, have total flux density > 100 mJy, and are not included in the core sample presented in Chapters 3 and 4. m_p =fractional linear polarization.

IAU name (B1950)	p (mJy)				m_p (%)			
	1.4	2.5	4.8	8.6	1.4	2.5	4.8	8.6
0219+428	86	40	41	50	6.3	3.1	3.6	4.9
0234+285	58	47	44	42	2.9	2.5	2.3	2.2
0446+112	5	8	6	8	0.6	1.0	0.7	0.7
0537-441	32	35	50	97	1.3	1.2	1.1	1.8
0546-642	1	< 1	< 1	1	0.9	< 0.2	< 0.2	0.5
0637-752	191	111	106	75	4.5	2.1	1.7	1.3
0735+178	17	20	19	18	1.4	1.7	1.7	1.8
0851+202	43	47	26	19	3.6	3.0	1.4	0.9
0912+297	7	8	7	6	2.4	3.6	3.7	3.7
1101+384	17	18	13	12	2.9	3.0	2.1	2.1
1215+303	23	25	24	19	6.3	6.8	6.1	4.8
1219+285	35	35	36	34	4.2	4.5	4.6	4.6
1510-089	59	25	26	45	2.7	1.3	1.4	2.6
1553+113	8	8	7	6	3.0	3.4	2.7	2.3
1633+382	29	26	17	18	1.0	1.0	0.7	0.8
1641+399	317	245	238	247	4.6	3.2	2.9	3.2
1652+398	41	47	47	41	2.5	3.0	3.0	2.8
1741+196	5	5	4	3	2.2	2.2	2.2	1.6
1749+096	38	52	70	215	3.3	2.8	2.2	5.6
2128-123	29	17	41	41	1.7	0.8	1.5	1.5
2200+420	178	209	194	164	4.4	5.2	4.9	4.1
2255-282	13	20	20	193	1.1	1.1	0.6	3.1